A study of growth and remodeling in isotropic tissues, based on the Anand-Aslan-Chester theory of strain-gradient plasticity

Received dd October 2018; | Revised dd Month Year; | Accepted dd Month Year

DOI: xxx/xxxx

ORIGINAL RESEARCH ARTICLE

A study of growth and remodelling in isotropic tissues, based on the Anand-Aslan-Chester theory of strain-gradient Plasticity.†

Alfio Grillo* | Salvatore Di Stefano | Ariel Ramírez-Torres | Michele Loverre

[1]Dipartimento di Scienze Matematiche (DISMA) "G. L. Lagrange", *'Dipartimento di Eccellenza 2018–2022'*, Politecnico di Torino, Torino, Italy

Correspondence
*Alfio Grillo, Corso Duca degli Abruzzi 24, I-10129, Torino (TO), Italy. Email: alfio.grillo@polito.it

Present Address
Corso Duca degli Abruzzi 24, I-10129, Torino (TO), Italy

Motivated by the increasing interest of the biomechanical community towards the employment of strain-gradient theories for solving biological problems, we study the growth and remodelling of a biological tissue on the basis of a strain-gradient formulation of remodelling. Our scope is to evaluate the impact of such an approach on the principal physical quantities that determine the growth of the tissue. For our purposes, we assume that remodelling is characterised by a coarse and a fine length scale and, taking inspiration from a work by L. Anand, O. Aslan, and S.A. Chester, we introduce a kinematic variable that resolves the fine scale inhomogeneities induced by remodelling. With respect to this variable, a strain-gradient framework of remodelling is developed. We adopt this formulation in order to investigate how a tumour tissue grows *and* how it remodels *in response* to growth. In particular, we focus on a type of remodelling that manifests itself in two different, but complementary, ways: on the one hand, it finds its expression in a stress-induced reorganisation of the adhesion bonds among the tumour cells, and, on the other hand, it leads to a change of shape of the cells and of the tissue, which is generally not recovered when external loads are removed. To address this situation, we resort to a generalised Bilby-Kröner-Lee decomposition of the deformation gradient tensor. We test our model on a benchmark problem taken from the literature, which we rephrase in two ways: micro-scale remodelling is disregarded in the first case, and accounted for in the second one. Finally, we compare and discuss the obtained numerical results.

KEYWORDS:
Growth, Remodelling, Strain-gradient Plasticity, Aifantis' theory

1 | INTRODUCTION

1.1 | A brief review on growth and remodelling

The growth of a biological tissue consists of the variation and redistribution of its mass, and is the consequence of processes that influence each other reciprocally in spite of their being characterised by different time and length scales [1–3].

Besides genetic, bio-chemical, and bio-physical phenomena, which pertain to the molecular and intra-cellular scales, the growth of a tissue also depends on interactions that occur at the inter-cellular level, as well as on those that involve the tissue as

†Submitted to the Special Issue ...

a whole. The latter two types of interactions are often studied with the purpose of describing how a tissue evolves, for instance, by adapting its internal structure and material properties in response to the changes of its environment.

In fact, the structural adaptation of a tissue may manifest itself in several different ways, and it may involve one or more classes of phenomena, which are often referred to with the common name of *remodelling*. For the types of problems addressed in this work, in which a tissue is viewed as an aggregate of cells, a reorganisation of its internal structure is assumed to occur through the dissolution and reformation of the adhesion bonds among the cells [4–6], or through a rearrangement of the position, shape, and orientation of the cells in the aggregate [7,8]. In both cases, remodelling acquires the character of a *configurational* process at the inter-cellular scale, and may result in an inelastic change of shape of the tissue as a whole. More generally, however, when the extracellular matrix (ECM) is accounted for, or in the case of fibre-reinforced tissues, the structural changes take place through the distortion of the ECM's collagenous network [9], or through the reorientation of the collagen fibres.

The problem of fibre reorientation has been addressed in several works, sometimes in connection with growth, and for different types of tissues, these ranging from blood vessels (see e.g. [10–13]) to articular cartilage (see e.g. [14–19]). In other situations, as is the case for bone, the concept of structural adaptation is introduced to interpret the formation of cracks [20], the onset of damage, and the occurrence of inelastic distortions that are remnant of the phenomenon of plasticity in metals (see e.g. [21,22]).

To describe the processes mentioned so far, a tissue may be viewed as a continuum, or a mixture of continua, and its dynamics may be revealed, at least *partially*, by formulating mathematical models based on the laws of continuum mechanics. Such models should capture the "two-level" nature of the phenomena that they are meant to resolve, thereby trying to connect the visible transformations of a tissue with the chemical, electrical, and mechanical interactions occurring inside it. For instance, in the case of growth, a connection of this kind is established by *mechanotransduction* [23,24], i.e., the modulation that mechanical stress exerts on the tissue's growth rate due to its interplay with the tissue's mass sources. Mechanotransduction has also been recently discussed by Ehret et al. [25] in the context of *"inverse poroelasticity"* for *"soft biomembranes"* and, in particular, in the case of the interplay between mechanical stress and chemical potential that results in the possibility of driving the variations of osmotic pressure through mechanical loading.

A number of papers has been produced in which growth and remodelling have been described by adopting the language and formalism of continuum theories (see e.g. [26] and the references therein). In some works devoted to the theoretical foundations of volumetric growth (see e.g. [27–29]), emphasis is put on the necessity of defining variables that, together with the descriptors of the tissue's *standard* mechanical state, are capable of catching its structural transformations. In [27], this is done by having recourse to the theory of uniformity [30,31], and introducing the concepts of *"archetype"* and *"transplant operator"* [27,30,31]. On the other hand, in several other contexts, the Bilby-Kröner-Lee multiplicative decomposition of the deformation gradient tensor is adopted, along with its generalisations, in order to frame remodelling in terms of "plastic-like distortions" (see e.g. [32]). We use this terminology in order to underline that, in the presence of remodelling, the structural transformations of the tissues considered in this work recall the plastic distortions of non-living, elasto-plastic materials. Sometimes, we use the adjectives "plastic" and "remodelling" interchangeably: we take this liberty when a physical quantity, historically conceived for the theory of plasticity, has to be re-interpreted in compliance with the physical context of the present work. A relevant example is the *accumulated plastic strain*, a variable for which we use both its original name and the name *accumulated remodelling strain*. In other cases, however, we use quotation marks for "plastic" and "plasticity", if we need to recall that we are borrowing terms from the theory of plasticity. For instance, we use this convention when we speak of *micro-scale plasticity*.

When a tissue is modelled as a mixture of continua —typically a fluid phase and one or more solid phases— [6,33–37], its growth is usually identified with an inter-phase exchange of mass. Such process is assumed to yield either an accretion of the solid mass at the expenses of the fluid or a loss of solid mass, induced by the disintegration of the tissue cells, which become necrotic and are then dissolved into the fluid. In such a framework, the solid phase is taken as a representation of the tissue cells (and, where appropriate, of the ECM), and a mathematical model of growth should be able to relate the mass variation of the solid phase with the availability of nutrients and with the structural transformations that possibly accompany growth. As already mentioned above, the latter ones are assumed to have inelastic nature and may refer to the redistribution of the solid mass, to the change of the cells' arrangement inside the tissue, so as to mimic the result of the dissolution and reformation of the cellular adhesion bonds, or to a combination of both phenomena.

To further clarify the type of remodelling addressed in this work, and to contextualise the wording "plastic-like distortions", we provide an explicit example of the inelastic rearrangement of the cells of a tissue. For this purpose, we discuss the results of an experiment commented in [8]. In Figure 1 (which corresponds to Figure 7 of [8]), Forgacs et al. [8] show three different stages of a cellular aggregate subjected to a loading history referred to as *"centrifugation"* [8]. The first column of Figure 1 reports the configuration of the aggregate *"before centrifugation"* [8], when the cells are *"isodiametric"* and the aggregate is spherical. The

second column, instead, shows the aggregate after a 5 minute centrifugation: at this stage, the aggregate is no longer spherical, the cells have changed their shape and are said to be in a *"rapidly relaxing, more elastic phase"*[8]. Finally, the third column depicts the configuration of the aggregate after 36 hour centrifugation. In this configuration, the aggregate is believed to have reached a new state of equilibrium, and its cells seem to have attained a state free of stress. Most importantly, the cells seem to have changed their positions and to have redistributed their shape and orientation in a permanent manner, so that the aggregate does not spontaneously tend to recover its original configuration, regardless of the absence of external loads. Forgacs et al.[8] use the theory of viscoelasticity to model the experiment described so far. To us, however, the inelastic behaviour of the cellular aggregate may also suggest interpretations other than, and perhaps complementary to, viscoelasticity. Indeed, looking at the third column of Figure 1 , one observes that the internal structure of the aggregate has changed, and this change seems to be due to the fact that the cells, relaxed or not, have modified their shape and arrangement inside the tissue. Therefore, at least in our opinion, viscoelasticity alone may be insufficient to accurately account for the irreversible deformations (distortions) of the tissue. Rather, the interpretation of the just discussed phenomenology may necessitate concepts borrowed from the theories of plasticity or viscoplasticity, since these are able to describe the tissue's internal kinematics in a way that is similar to the motion of the defects in solids. This view seems to be corroborated also by other experiments conducted on tumour spheroids (see e.g.[38] and references therein). In such experiments, a spheroid is allowed to grow and, after growth has occurred, it is cut radially for a length of about the 80% of its diameter: what is observed is a relaxation of the stresses, resulting in the opening of the spheroid, with the edges of the cut drifting away from one another (see Figure 1 d). This behaviour, in fact, suggests the existence of an incompatible, stress-free state of the tumour, which is consistent with the description of the tumour as an elasto-plastic material. To us, this observation justifies the approach followed in our work, although it does not exclude visco-plastic effects. While bearing this in mind, for simplicity we restrict here our investigations to the case of plasticity alone, and we adopt this approach to model the internal rearrangement, i.e., the remodelling, of the tissues studied in our work.

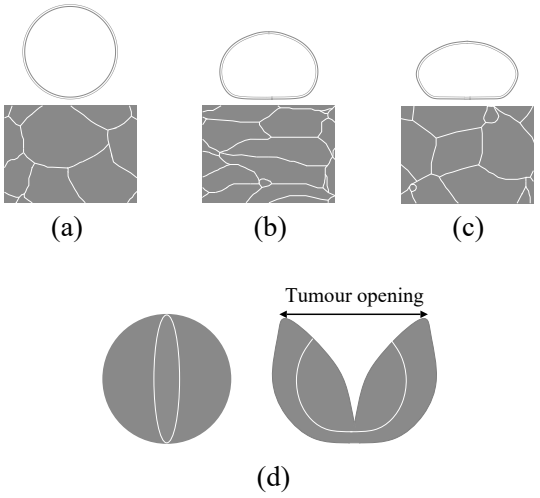

FIGURE 1 First row (redrawn and adapted from Forgacs et al.[8]): Schematic representation of the cells rearrangement in an spherical aggregate (a) before centrifugation, (b) after a 5 minute centrifugation, and (c) after 36 hour centrifugation. Second row (redrawn and adapted from Stylianopoulos et al.[38]): Stress relaxation of a tumour spheroid after a radial cut is performed.

Understanding how growth and remodelling are related to each other is a necessary step towards the comprehension of the evolution of biological tissues. In this respect, we remark that the coupling of growth and remodelling has been investigated in several papers (see e.g.[4,24,37] and the references therein, without considering strain-gradient constitutive laws, while second-order theories have been proposed e.g. by Ciarletta et al.[39–41] to investigate the transport of mass in the presence of morphogenesis (see also[27] for a discussion on this issue).

To move forward in the comprehension of how growth and remodelling interact, an important question to answer is how to relate mechanical stress with both phenomena (see e.g.[26,42]). For example, the tearing of the inter-cellular bonds in a tumour, which can be interpreted as an expression of remodelling[4,5], leads to the relaxation of stress, and stress, apart from mechano-transduction, may play a role on the growth of the tumour. Indeed, a recent result of some of us seems to show that remodelling

enhances the growth of a tumour in the avascular stage by increasing the speed at which the tumour's boundary advances in space[24]. Although this result necessitates validations, it may help to estimate qualitatively a possible interplay between remodelling and growth. To this end, Mascheroni et al.[24],drew the conclusion that the observed behaviour was the consequence of the smoothing effect of the plastic-like distortions on mechanical stress, and that such effect was transferred to the term describing growth through the mechanotransduction.

The type of remodelling induced by mechanical stress can be viewed as a plastic-like behaviour and, if one assumes plastic response to be triggered by a yield stress (as is the case, for instance, in rate-independent[22,43] or in Perzyna-like plasticity[22]), one may conclude that remodelling commences in the regions of the tissue in which the stress exceeds a certain threshold. Since in a growing tissue such regions are those in which the growth is predominant and the deformation is inhibited, it is very important to resolve accurately the plastic-like distortions. This exigency becomes stringent when the "plastic" strains accumulate in very narrow zones. In such cases, a useful tool of investigation could be to switch from a local to a *"non-local"* model of plasticity. A possible way of accomplishing this task is supplied by the theory proposed by Anand et al. in[44]. However, before exposing such theory and adapting it to our purposes, we should clarify that the framework within which Anand et al.[44–46] and Gurtin et al.[45] developed their work is deeply different from ours. Indeed, the *"gradient regularisation"* presented in their paper is introduced for numerical reasons, that is, with the purpose of correctly resolving the accumulated plastic strain in the shear bands that arise in strain-softening materials. Anand et al.[44] justify such regularisation by means of the concept of *"micro-scale plasticity"* and, by doing this, they actually admit the existence of a physics that cannot be captured by standard theories of plasticity. The Authors, in fact, end up with a yield condition expressed by a partial differential equation in the variable that resolves the fine scale remodelling (*"micro-plasticity"*, in the jargon of Anand et al.[44]). Such equation resolves the length scale over which the plastic strain is accumulated, and allows to recover a yield condition in the style of Aifantis[47,48]. Starting from the approach suggested by Anand et al.[44], and in spite of the differences between their framework and ours, we investigate how the introduction of a fine scale remodelling affects our growth problem.

1.2 | Aim of our work

The main goal of our work is to determine the consequences of a strain-gradient formulation of remodelling on the growth of a biological tissue. Many different paths could be followed to address this question. Indeed, one may adopt the framework developed in[27], in which a constitutive theory is developed that features the first- and second-order gradient of the deformation as well as the first- and second-order *"transplant operators"*[39–41]. Alternatively, one may turn to a gradient theory of remodelling in continua with micro-structure by elaborating the Cosserat-type approach put forward in[31]. Another possibility is to have recourse to the higher-order gradient theories presented, for example, by[49] for the case of partially saturated porous media, and by[50] for problems of bone reconstruction (see also[51] for a review).

In this work, we focussed on the approach based on the *"micro-scale plasticity"* of Anand et al.[44] because of its "simplicity". This approach, indeed, is "simple" because it describes the phenomenon of micro-plasticity by means of a *scalar* variable, which makes its use and implementation rather straightforward in the study of growth and remodelling as coupled phenomena.

As explained by[44], the micro-scale plasticity describes the inhomogeneities that arise, in the plastic regions of a material, at a length scale much smaller than the one at which the standard accumulated plastic strains are resolved. According to the theory of Anand et al.[44,46], and similarly to what is done in Gurtin[52] and by Gurtin and Anand[45], the micro-scale plasticity is investigated by enriching the standard kinematics that describes an elasto-plastic body. In this respect, a dedicated kinematic descriptor is introduced, whose task is to capture the fine scale plastic inhomogeneities, and, along with it, a force balance equation is added to the list of balance laws of a classical elasto-plastic problem. Such additional force balance is deduced by the means of the Principle of Virtual Powers and, under suitable hypotheses, the forces featuring in it can be obtained constitutively by exploiting the dissipation inequality of the considered system.

For our purposes, we consider a benchmark problem taken from the literature[53,54], and we adapt it to our framework. We elaborate two different formulations of this problem. In the first one, referred to as "standard model" (or approach), we give no room to micro-scale "plasticity", and we adopt the accumulated "plastic" strain, denoted by ε_p, as the only measure of the plastic-like distortions representing the tissue's remodelling. In the second formulation, referred to as "non-standard model", we switch on the micro-scale "plasticity" and, as done by[44], we assume that the information about this type of fine scale remodelling is disclosed by a scalar variable, denoted by $\mathfrak{e}_p$. Then, the difference between $\mathfrak{e}_p$ and ε_p indicates to what extent remodelling tends to be a two-scale phenomenon.

We emphasise that our leading motivation is to weigh the influence of the strain-gradient approach outlined above on the main descriptors of growth in the considered benchmark problem.

1.3 | Limitations and novelties

Once that our work plan is explained, we recall that, as is known from the literature, the non-standard approach is necessary for materials exhibiting strain-softening elasto-plastic behaviour, and when the plastic distortions tend to be markedly localised. The occurrence of the strain-softening behaviour is related to the definition of the yield stress of the considered material, expressed as a monotonically decreasing function of the accumulated plastic strain, whereas the localisation of plastic strains may be strongly problem dependent. Before going further, we should thus clarify that, to the best of our knowledge, no strain-softening behaviour has been observed in the biological tissues under investigation: it might occur or not, and, if it occurs, it is not necessarily ascribable to the accumulated plastic strain. Moreover, in the problem analysed in the sequel, the localisation of the accumulated "plastic" strain is not so pronounced to call at all costs for the non-standard approach. It should also be mentioned that the type of remodelling addressed in our work cannot be employed, as it stands, for any kind of biological tissue. In fact, our model might be adequate for tumours [4], as it describes stress-driven irreversible deformations, which are related to a rearrangement of the cells' shape and of the cellular adhesion network. However, it is very likely inappropriate for tissues capable of bearing loads, such as tendons and blood vessels. For such tissues, indeed, the occurrence of remodelling is put in relation to *"tensional homeostasis"* [55]. Furthermore, we can speak of "irreversibility" only for processes occurring over relatively short time windows. Indeed, even though plastic-like distortions take place, the tissue may recover its initial shape because cells grow or because the cells move actively towards their original configuration. In addition to these considerations, we clarify that, in this work, we study only the case in which growth is inhibited by the lack of nutrients or boosted by their consumption. This hypothesis is typical for tumours, in which cells thrive as long as nourishment is at their disposal. However, more generally, and especially in tissues other than tumours, nutrients are not the only agents responsible for cell proliferation. The latter, indeed, can be repressed or enhanced, depending, for instance, on the presence of physical barriers, lack of space, or the occurrence of contact inhibition mechanisms.

In spite of the limitations outlined above, our approach offers some essential novelties that can improve the interpretation of benchmark problems in which the accumulated remodelling strain is sufficiently localised. This could be the case when the growth of a tissue is strongly promoted by a great availability of nutrients, while its deformation is prohibited by the presence of constraints, like undeformable walls or contact with much stiffer materials. In such situations, indeed, the mechanical stress increases and, when it overcomes a given threshold, a plastic-like remodelling is activated. In the cases in which a confinement of the accumulated "plastic" strain takes place, e.g. close to an interface separating two materials or at the constrained boundaries of a tissue, the non-standard approach proposed in our work can help to achieve a better resolution of its growth and remodelling.

More in detail, the novelties of the present study with respect to previous publications of some of us [24,54] are the following: (i) we analyse the coupling between growth and remodelling both theoretically and computationally, and we resolve the remodelling at two different length scales; (ii) with the aid of the theory developed by Anand et al. [44], we formulate remodelling within a strain-gradient framework, thereby generalising our past approaches, which were of "grade zero" in the remodelling variables[1].

Furthermore, the major novelties of our contribution with respect to the work of Anand et al. [44] are the following: (a) in our work, the material is a biphasic medium, featuring a solid and a fluid phase, with the solid phase comprising two populations of cells, and the fluid carrying chemical substances; (b) the interplay between growth and remodelling leads to several interactions that are accounted for in several parts of the mathematical model, and that address, for instance, the evolution of the fluid pressure, of the nutrients, and of the cell populations. Moreover, with reference to point (b), we emphasise the generalisation of the equation for the micro-scale plasticity [44], in which the length associated with the spatial evolution of $\mathbf{e}_p$, rather than being a constant (cf. [44]), depends on growth and on the coarse scale plastic-like distortions.

[1] We remark that, in Grillo et al. [18] and Crevacore et al. [19], we do present a first grade theory for the considered remodelling variable, but such variable does not represent plastic-like distortions. Rather, it is the order parameter describing the mean fibre orientation in a fibre-reinforced biological tissue.

2 | THEORETICAL BACKGROUND

The problem under investigation involves the motion of the solid phase, the motion of the fluid phase, the distortions related to growth, and plastic-like distortions, which are associated with the reorganisation of the tissue's internal structure. The definitions supplied in this section can be encountered in many works addressing Mixture Theory, and have been recently used for establishing the theoretical framework of previous works of some of us[18,19,54,56]. Such framework, in turn, has been adapted from the kinematic description of biphasic mixtures as developed by Quiligotti[57] and Quiligotti et al.[58].

2.1 | Mass balance laws

Following Mascheroni et al.[24] and Di Stefano et al.[54], the solid phase of the tissue is assumed to comprise only two types of cells, i.e., the proliferating cells and the necrotic ones. Their presence in the tissue is measured by the mass densities $\varphi_s\rho_s c_p$ and $\varphi_s\rho_s c_n$, respectively, where φ_s is the volumetric fraction of the solid phase, ρ_s is its true mass density, while c_p and c_n are the cells' mass fractions, compelled to satisfy the constraint $c_p + c_n = 1$, everywhere in $\mathscr{C}_t$ and $\mathscr{I}$. Here, $\mathscr{I} \subset \mathbb{R}$ is an interval of time, and $\mathscr{C}_t$ is the subset of the three-dimensional Euclidean space, $\mathscr{S}$, occupied by the biphasic system at time t. Note that the indices "p" and "n" stand for "proliferating" and "necrotic", respectively. Once the composition of the solid phase is specified, it is possible to characterise the mass balance of the solid phase by writing one balance law for each cell population, i.e.,

$$\partial_t(\varphi_s\rho_s c_p) + \operatorname{div}(\varphi_s\rho_s c_p \boldsymbol{v}_s) = r_{fp} + r_{pn} + r_{p\gamma}, \tag{1a}$$

$$\partial_t(\varphi_s\rho_s c_n) + \operatorname{div}(\varphi_s\rho_s c_n \boldsymbol{v}_s) = r_{nf} - r_{pn} + r_{n\gamma}. \tag{1b}$$

As reported by Mascheroni et al.[24] and Di Stefano et al.[54], r_{fp} describes the transfer of mass from the fluid phase to the solid phase, r_{nf} measures the dissolution per unit time of the necrotic cells in the fluid, r_{pn} is the rate at which the proliferating cells become necrotic, and the last two terms $r_{p\gamma}$ and $r_{n\gamma}$ have been introduced Di Stefano et al.[54] to evaluate how the growth-induced structural transformations of the tissue influence the local density changes of the solid constituents. Both terms, however, are assumed to be identically zero in the present work. Equations (1a) and (1b) have been obtained under the assumption that both the proliferating and the necrotic cells move with the velocity of the solid phase, $\boldsymbol{v}_s$. Moreover, because of the constraint on the mass fractions, they can be rephrased as

$$\partial_t(\varphi_s\rho_s c_p) + \operatorname{div}(\varphi_s\rho_s c_p \boldsymbol{v}_s) = r_{pn} + r_{fp}, \tag{2a}$$

$$\partial_t(\varphi_s\rho_s) + \operatorname{div}(\varphi_s\rho_s \boldsymbol{v}_s) = r_{fp} + r_{nf} \equiv r_s. \tag{2b}$$

Note that the last equality of Equation (2b) defines the overall source/sink of mass of the solid phase, i.e., the term r_s, which describes the variation of the tissue's mass due to growth.

Finally, we relate the occurrence of growth with the presence of nutrients in the tissue. These are conveyed by the fluid phase to the proliferating cells and are believed to activate or inhibit growth depending on whether or not they exceed a certain threshold. To characterise the evolution of the nutrients, we introduce the *nutrients' mass fraction*, c_N, and the mass density $\varphi_f\rho_f c_N$, where φ_f and ρ_f indicate the volumetric fraction and the mass density of the fluid phase, respectively. In addition, we require that the tissue obeys the saturation condition, i.e., $\varphi_f = 1 - \varphi_s$, and we consider the mass balance laws of the nutrients and of the fluid phase as a whole, i.e.[24,54],

$$\partial_t(\varphi_f\rho_f c_N) + \operatorname{div}(\varphi_f\rho_f c_N \boldsymbol{v}_f + \boldsymbol{y}_N) = r_{Np}, \tag{3a}$$

$$\partial_t(\varphi_f\rho_f) + \operatorname{div}(\varphi_f\rho_f \boldsymbol{v}_f) = -r_s. \tag{3b}$$

In (3a) and (3b), $\boldsymbol{v}_f$ is the velocity of the fluid phase, $\boldsymbol{y}_N$ is the mass flux vector associated with the motion of the nutrients relative to $\boldsymbol{v}_f$, r_{Np} is the rate at which the nutrients are consumed by the proliferating cells, and the right-hand-side of (3b) is taken equal to the negative of r_s in order to ensure the local conservation of mass for the biphasic mixture under study.

Next, we hypothesise that the mass densities of the solid and of the fluid phase can be regarded as constants in the range of interest for the problem at hand. Hence, we set $\rho_s(x,t) = \rho_{s0}$ and $\rho_f(x,t) = \rho_{f0}$ for all $x \in \mathscr{C}_t$ and $t \in \mathscr{I}$, and we summarise (2a), (2b), (3a), and (3b) in the following system of equations

$$\varphi_s\rho_{s0}\mathrm{D}_s c_p = r_{pn} + r_{fp} - r_s c_p, \tag{4a}$$

$$\rho_{s0}\mathrm{D}_s\varphi_s + \rho_{s0}\varphi_s \operatorname{div}\boldsymbol{v}_s = r_s, \tag{4b}$$

$$\varphi_f\rho_{f0}\mathrm{D}_s c_N + \varphi_f\rho_{f0}\boldsymbol{w}\,\nabla c_N + \operatorname{div}\boldsymbol{y}_N = r_{Np} + r_s c_N, \tag{4c}$$

$$\operatorname{div}\boldsymbol{v}_{\mathrm{s}} + \operatorname{div}(\varphi_{\mathrm{f}}\boldsymbol{w}) = \left(\frac{1}{\rho_{\mathrm{s0}}} - \frac{1}{\rho_{\mathrm{f0}}}\right) r_{\mathrm{s}}, \tag{4d}$$

where, for any given physical quantity f, the symbol $\mathrm{D}_{\mathrm{s}} f \equiv \partial_t f + (\nabla f)\boldsymbol{v}_{\mathrm{s}}$ denotes the substantial derivative of f with respect to the solid phase velocity, and $\boldsymbol{w} \equiv \boldsymbol{v}_{\mathrm{f}} - \boldsymbol{v}_{\mathrm{s}}$ is the velocity of the fluid relative to the solid. Note that the product $\varphi_{\mathrm{f}}\boldsymbol{w}$ is often referred to as *filtration velocity*[59], although it actually represents a specific mass flux vector[60].

For future use, we remark that the mass balance law (4d) can also be recast in the equivalent representation

$$\varphi_{\mathrm{s}}\operatorname{div}\boldsymbol{v}_{\mathrm{s}} + \varphi_{\mathrm{f}}\operatorname{div}\boldsymbol{v}_{\mathrm{f}} + (\nabla\varphi_{\mathrm{f}})\boldsymbol{w} = \left(\frac{1}{\rho_{\mathrm{s0}}} - \frac{1}{\rho_{\mathrm{f0}}}\right) r_{\mathrm{s}}. \tag{5}$$

2.2 | Kinematics

The motion of the solid phase is described by the smooth mapping $\chi : \mathscr{B} \times \mathscr{I} \to \mathscr{S}$, where $\mathscr{B}$ is the tissue's reference configuration. For each pair $(X,t) \in \mathscr{B} \times \mathscr{I}$, the spatial point occupied by the solid phase is given by $x = \chi(X,t) \in \mathscr{S}$. By differentiating χ with respect to its arguments, we obtain the deformation gradient tensor, i.e., the tangent map of χ, defined by $\boldsymbol{F}(X,t) = T\chi(X,t) : T_X\mathscr{B} \to T_{\chi(X,t)}\mathscr{S}$[61], and the solid phase velocity $\boldsymbol{V}_{\mathrm{s}}(X,t) = \dot{\chi}(X,t)$. Here, $T_X\mathscr{B}$ and $T_{\chi(X,t)}\mathscr{S}$ are the tangent space of $\mathscr{B}$ at X and the tangent space of $\mathscr{S}$ at $\chi(X,t)$, respectively[61], and the superimposed dot means partial differentiation with respect to time. For completeness, we recall the relationship between $\boldsymbol{V}_{\mathrm{s}}$ and the Eulerian velocity of the solid phase, i.e., $\boldsymbol{v}_{\mathrm{s}}(x,t) = \boldsymbol{v}_{\mathrm{s}}(\chi(X,t),t) = \boldsymbol{V}_{\mathrm{s}}(X,t)$, so that the composition $\boldsymbol{v}_{\mathrm{s}}(\,\cdot\,,t)\circ\chi(\,\cdot\,,t) = \boldsymbol{V}_{\mathrm{s}}(\,\cdot\,,t)$ holds true for all $t \in \mathscr{I}$.

The fluid motion is described by the Eulerian velocity $\boldsymbol{v}_{\mathrm{f}}(x,t)$, evaluated at every point $x \in \mathscr{S}$ occupied by the fluid and at time $t \in \mathscr{I}$. Note that, since the system under investigation is a mixture, the fluid co-exists with the solid at every point $x \in \mathscr{S}$ at which the tissue is observed. Thus, the point x can also be viewed as the image of X through the solid motion, i.e., $x = \chi(X,t)$, and the fluid motion can be studied by means of the composition $\boldsymbol{V}_{\mathrm{f}}(\,\cdot\,,t) \equiv \boldsymbol{v}_{\mathrm{f}}(\,\cdot\,,t)\circ\chi(\,\cdot\,,t)$, such that $\boldsymbol{V}_{\mathrm{f}}(X,t) = \boldsymbol{v}_{\mathrm{f}}(\chi(X,t),t)$.

To account for the growth and structural reorganisation of the tissue, we have recourse to the multiplicative decomposition of the deformation gradient tensor, which we propose in the form[4,37,62]

$$\boldsymbol{F} = \boldsymbol{F}_{\mathrm{e}}\boldsymbol{F}_{\mathrm{p}}\boldsymbol{F}_{\gamma}. \tag{6}$$

In (6), $\boldsymbol{F}_{\gamma}$, $\boldsymbol{F}_{\mathrm{p}}$, and $\boldsymbol{F}_{\mathrm{e}}$ describe the distortions associated with the uptake or loss of mass, the distortions accompanying the plastic-like rearrangement of the tissue's internal structure, and the distortions due to the elastic accommodation of the tissue, respectively. In the sequel, $\boldsymbol{F}_{\mathrm{p}}$ and $\boldsymbol{F}_{\gamma}$ will also be referred to as *remodelling tensor*[2] and *growth tensor*, respectively. We notice that, whereas it is rather standard to consider $\boldsymbol{F}_{\mathrm{e}}$ as the first factor of the right-hand-side of (6), the order of appearance of $\boldsymbol{F}_{\mathrm{p}}$ and $\boldsymbol{F}_{\gamma}$ is not standard at all. Indeed, it is conceivable to formulate a decomposition of $\boldsymbol{F}$ in which the inelastic contributions to the overall deformation appear in reverse order. In addition, there exist also cases in which the accommodating part of the deformation is put at the end of the decomposition[63]. We adopt the order shown above because, in the present work, we have in mind a tissue that grows *and* that remodels its internal structure *in response* to growth. This statement notwithstanding, we regard growth and structural reorganisation as independent, yet mutually interacting processes. Consequently, we consider $\boldsymbol{F}_{\mathrm{p}}$ and $\boldsymbol{F}_{\gamma}$ as independent kinematic (tensor) variables and, following the same philosophy outlined in some previous publications[13,19,29,36,54,64], we associate each of them with degrees of freedom having the same "dignity" as those related to the other kinematic descriptors, i.e., $\boldsymbol{V}_{\mathrm{s}}$ and $\boldsymbol{V}_{\mathrm{f}}$. Finally, we emphasise that the decomposition (6) is a generalised Bilby-Kröner-Lee decomposition (see e.g. Mićunović[22] for similar decompositions in the case of damage or other inelastic processes). Since we have recently discussed the decomposition (6) in Di Stefano[54] for the case of growth, here we do not fuss over the physics behind it, and we suggest the reviews[22,65] for details. However, we recall that, for every $X \in \mathscr{B}$ and $t \in \mathscr{I}$, the product $\boldsymbol{F}_{\mathrm{p}}(X,t)\boldsymbol{F}_{\gamma}(X,t)$ maps vectors of the tangent space $T_X\mathscr{B}$ into vectors of the image vector space $\mathscr{N}_t(X)$, attached at X. By ideally performing such transformation for all $X \in \mathscr{B}$, the solid phase is brought into a relaxed state at time t, the latter being characterised by the absence of *any* stresses, including the residual ones. Such state is also referred to as *natural state*[22,66].

Differentiation of $\boldsymbol{F}$ with respect to time and left-multiplication by $\boldsymbol{F}^{-1} = \boldsymbol{F}_{\gamma}^{-1}\boldsymbol{F}_{\mathrm{p}}^{-1}\boldsymbol{F}_{\mathrm{e}}^{-1}$ yield

$$\dot{\boldsymbol{F}}\boldsymbol{F}^{-1} = \dot{\boldsymbol{F}}_{\mathrm{e}}\boldsymbol{F}_{\mathrm{e}}^{-1} + \boldsymbol{F}_{\mathrm{e}}\boldsymbol{L}_{\mathrm{p}}\boldsymbol{F}_{\mathrm{e}}^{-1} + \boldsymbol{F}_{\mathrm{e}}\boldsymbol{F}_{\mathrm{p}}\boldsymbol{L}_{\gamma}\boldsymbol{F}_{\mathrm{p}}^{-1}\boldsymbol{F}_{\mathrm{e}}^{-1}, \tag{7}$$

[2] We use the subscript "p" to emphasise the fact that the distortions associated with remodelling are plastic-like. In this respect, we could have also referred to $\boldsymbol{F}_{\mathrm{p}}$ as "plasticity tensor". However, we prefer to speak here of "remodelling tensor", because the concept of remodelling is more specific for the addressed biological materials.

where we introduced the tensor of *rate of remodelling-induced distortions*, $\boldsymbol{L}_{\mathrm{p}} \equiv \dot{\boldsymbol{F}}_{\mathrm{p}}\boldsymbol{F}_{\mathrm{p}}^{-1}$, and the tensor of *rate of growth-induced distortions*, $\boldsymbol{L}_{\gamma} \equiv \dot{\boldsymbol{F}}_{\gamma}\boldsymbol{F}_{\gamma}^{-1}$. In compliance with (6), the *volume ratio* $J \equiv \det \boldsymbol{F}$ can be rewritten as $J = J_{\mathrm{e}}J_{\mathrm{p}}J_{\gamma}$, where $J_{\mathrm{e}} \equiv \det \boldsymbol{F}_{\mathrm{e}}$, $J_{\mathrm{p}} \equiv \det \boldsymbol{F}_{\mathrm{p}}$, and $J_{\gamma} \equiv \det \boldsymbol{F}_{\gamma}$ denote, respectively, the volumetric distortions associated with the elastic, remodelling, and growth part of the deformation gradient tensor. We use these definitions to perform the Piola transformations of (4a)–(4d), thereby obtaining

$$\rho_{\mathrm{s}0}\Phi_{\mathrm{s}}\dot{\omega}_{\mathrm{p}} = R_{\mathrm{pn}} + R_{\mathrm{fp}} - R_{\mathrm{s}}\omega_{\mathrm{p}}, \tag{8a}$$

$$\rho_{\mathrm{s}0}\dot{\Phi}_{\mathrm{s}} = R_{\mathrm{s}}, \tag{8b}$$

$$\rho_{\mathrm{f}0}\Phi_{\mathrm{f}}\dot{\omega}_{\mathrm{N}} + \rho_{\mathrm{f}0}\boldsymbol{Q}\,\mathrm{Grad}\,\omega_{\mathrm{N}} + \mathrm{Div}\boldsymbol{Y}_{\mathrm{N}} = R_{\mathrm{Np}} + R_{\mathrm{s}}\omega_{\mathrm{N}}, \tag{8c}$$

$$\dot{J} + \mathrm{Div}\,\boldsymbol{Q} = \left(\frac{1}{\rho_{\mathrm{s}0}} - \frac{1}{\rho_{\mathrm{f}0}}\right) R_{\mathrm{s}}, \tag{8d}$$

where, for every $X \in \mathscr{B}$ and $t \in \mathscr{I}$, we denote by

$$\Phi_{\alpha}(X,t) = J(X,t)\varphi_{\alpha}(\chi(X,t),t), \qquad \alpha \in \{\mathrm{f},\mathrm{s}\}, \tag{9a}$$

$$R_{\beta}(X,t) = J(X,t)r_{\beta}(\chi(X,t),t), \qquad \beta \in \{\mathrm{pn},\mathrm{fp},\mathrm{s},\mathrm{Np}\}, \tag{9b}$$

$$\omega_{\upsilon}(X,t) = c_{\upsilon}(\chi(X,t),t), \qquad \upsilon \in \{\mathrm{p},\mathrm{N}\}, \tag{9c}$$

the material volumetric fractions, the material sources/sinks of mass, and the mass fractions expressed as functions of X and time, respectively. Moreover, we introduced the material flux vectors associated with the filtration velocity $\varphi_{\mathrm{f}}\boldsymbol{w}$ and with the nutrients' mass flux vector $\boldsymbol{y}_{\mathrm{N}}$, respectively, i.e.,

$$\boldsymbol{Q}(X,t) = \Phi_{\mathrm{f}}(X,t)\boldsymbol{w}(\chi(X,t),t)\boldsymbol{F}^{-\mathrm{T}}(X,t), \tag{10a}$$

$$\boldsymbol{Y}_{\mathrm{N}}(X,t) = \boldsymbol{J}(X,t)[\boldsymbol{y}_{\mathrm{N}}(\chi(X,t),t)]\boldsymbol{F}^{-\mathrm{T}}(X,t). \tag{10b}$$

In particular, $\boldsymbol{Q}$ will also be referred to as *material filtration velocity* in the sequel.

The kinematic picture of the problem under study is completed with a scalar descriptor, denoted by $\mathrm{e}_{\mathrm{p}} : \mathscr{C}_t \times \mathscr{I} \to \mathbb{R}$. This quantity and its gradient, $\nabla \mathrm{e}_{\mathrm{p}}$, have been introduced by[44] with the purpose of constructing indicators of the inelastic transformations occurring in the body at the scale of its micro-structure. More precisely, Anand et al.[44] speak of e_{p} in terms of a *"measure of the inhomogeneity of the microscale plasticity"*. In our framework, it is more appropriate to interpret e_{p} as a variable defined to resolve explicitly the inhomogeneities induced by the remodelling of the tissue. To this end, we define the "Lagrangian field" $\mathfrak{e}_{\mathrm{p}}$, such that $\mathfrak{e}_{\mathrm{p}}(X,t) = \mathrm{e}_{\mathrm{p}}(\chi(X,t),t)$, and the material gradient $\mathrm{Grad}\mathfrak{e}_{\mathrm{p}}(X,t) = [\nabla \mathrm{e}_{\mathrm{p}}(\chi(X,t),t)]\boldsymbol{F}(X,t)$.

2.3 | Constraints on the kinematic variables

By virtue of the presence of growth in our model, the study conducted in this work may be thought of as a slight generalisation of the framework depicted by Anand et al.[44], where the Authors develop a scalar theory of strain-gradient plasticity based on several *ab initio* restrictions on the kinematic variables of their problem. Such restrictions are expressed in terms of the generalised velocities of the proposed theory, and are thus cast in non-holonomic form. To highlight their role on the overall dynamics of the system under investigation, we specify the imposed constraints, and we discuss in detail their impact on the kinematic descriptors that they involve.

For the sake of clarity, we start with rephrasing, in our formalism, the constraints on $\boldsymbol{F}_{\mathrm{p}}$ and $\dot{\boldsymbol{F}}_{\mathrm{p}}$ introduced by Anand et al.[44]. On the top of those, we exploit the mass balance laws in order to extract pieces of information that can be interpreted as constraints on the growth tensor, $\boldsymbol{F}_{\gamma}$, and on its rate $\boldsymbol{L}_{\gamma}$.

If $\boldsymbol{L}_{\mathrm{p}}$ is assigned, $\boldsymbol{F}_{\mathrm{p}}$ can be computed by integrating the ordinary differential equation $\dot{\boldsymbol{F}}_{\mathrm{p}} = \boldsymbol{L}_{\mathrm{p}}\boldsymbol{F}_{\mathrm{p}}$, which can be rewritten as

$$\dot{\boldsymbol{F}}_{\mathrm{p}} = \left(\boldsymbol{\eta}^{-1}\boldsymbol{D}_{\mathrm{p}} + \boldsymbol{\eta}^{-1}\boldsymbol{W}_{\mathrm{p}}\right)\boldsymbol{F}_{\mathrm{p}}, \tag{11}$$

where $\boldsymbol{\eta}$ is the metric tensor associated with the tissue's natural state, while $\boldsymbol{D}_{\mathrm{p}}$ and $\boldsymbol{W}_{\mathrm{p}}$ are the symmetric part and the skew-symmetric part of $\boldsymbol{L}_{\mathrm{p}}$, respectively, i.e.,

$$\boldsymbol{D}_{\mathrm{p}} = \mathrm{sym}(\boldsymbol{\eta}\boldsymbol{L}_{\mathrm{p}}) = \tfrac{1}{2}\left(\boldsymbol{\eta}\boldsymbol{L}_{\mathrm{p}} + \boldsymbol{L}_{\mathrm{p}}^{\mathrm{T}}\boldsymbol{\eta}\right), \tag{12a}$$

$$\boldsymbol{W}_{\mathrm{p}} = \mathrm{skew}(\boldsymbol{\eta}\boldsymbol{L}_{\mathrm{p}}) = \tfrac{1}{2}\left(\boldsymbol{\eta}\boldsymbol{L}_{\mathrm{p}} - \boldsymbol{L}_{\mathrm{p}}^{\mathrm{T}}\boldsymbol{\eta}\right). \tag{12b}$$

Following the theory of[44], the *first constraint* on $\boldsymbol{F}_\mathrm{p}$ is supplied by requiring from the outset that the *"plastic" spin tensor*, $\boldsymbol{W}_\mathrm{p}$ vanishes identically, i.e., $\boldsymbol{W}_\mathrm{p} = \boldsymbol{0}$. Hence, we obtain the identity $\boldsymbol{L}_\mathrm{p} = \boldsymbol{\eta}^{-1}\boldsymbol{D}_\mathrm{p}$, and, consequently, Equation (11) becomes

$$\dot{\boldsymbol{F}}_\mathrm{p} = \boldsymbol{\eta}^{-1}\boldsymbol{D}_\mathrm{p}\boldsymbol{F}_\mathrm{p}. \tag{13}$$

The *second constraint* on $\boldsymbol{F}_\mathrm{p}$ stems from the hypothesis of isochoric remodelling distortions, i.e., $J_\mathrm{p} = \det \boldsymbol{F}_\mathrm{p} = 1$. This relation, in turn, can be put in differential form, i.e., $\dot{J}_\mathrm{p} = J_\mathrm{p}\mathrm{tr}[\dot{\boldsymbol{F}}_\mathrm{p}\boldsymbol{F}_\mathrm{p}^{-1}] = 0$, and implies $\mathrm{tr}[\boldsymbol{\eta}^{-1}\boldsymbol{D}_\mathrm{p}] = 0$, as can be deduced by right-multiplying Equation (13) by $\boldsymbol{F}_\mathrm{p}^{-1}$ and taking the trace of the resulting expression. Accordingly, only the deviatoric part of $\boldsymbol{D}_\mathrm{p}$, i.e., $\tilde{\boldsymbol{D}}_\mathrm{p} = \boldsymbol{D}_\mathrm{p} - \frac{1}{3}\mathrm{tr}[\boldsymbol{\eta}^{-1}\boldsymbol{D}_\mathrm{p}]\boldsymbol{\eta}$, is involved in (13), which reduces to

$$\dot{\boldsymbol{F}}_\mathrm{p} = \boldsymbol{\eta}^{-1}\tilde{\boldsymbol{D}}_\mathrm{p}\boldsymbol{F}_\mathrm{p}. \tag{14}$$

In analogy with[44], we base our model on the further hypothesis that $\tilde{\boldsymbol{D}}_\mathrm{p}$ is *co-directional* with a tensor $\boldsymbol{N}_\nu$, associated with the tissue's natural state, and obtained by normalising a symmetric tensorial measure of stress, which will be specified later. In formulae, by indicating with $\boldsymbol{\Sigma}_\nu$ such measure of stress, we define $\boldsymbol{N}_\nu$ as

$$\boldsymbol{N}_\nu \equiv \frac{\boldsymbol{\eta}\tilde{\boldsymbol{\Sigma}}_\nu\boldsymbol{\eta}}{\|\tilde{\boldsymbol{\Sigma}}_\nu\|_{\boldsymbol{\eta}}}, \tag{15}$$

where $\tilde{\boldsymbol{\Sigma}}_\nu \equiv \boldsymbol{\Sigma}_\nu - \frac{1}{3}\mathrm{tr}[\boldsymbol{\eta}\boldsymbol{\Sigma}_\nu]\boldsymbol{\eta}^{-1}$ is the deviatoric part of $\boldsymbol{\Sigma}_\nu$, and $\boldsymbol{\eta}\tilde{\boldsymbol{\Sigma}}_\nu\boldsymbol{\eta}$ is the covariant representation of $\tilde{\boldsymbol{\Sigma}}_\nu$, and we enforce the co-directionality condition as the *third constraint* on $\boldsymbol{F}_\mathrm{p}$, i.e.,

$$\tilde{\boldsymbol{D}}_\mathrm{p} = \|\tilde{\boldsymbol{D}}_\mathrm{p}\|_{\boldsymbol{\eta}^{-1}}\boldsymbol{N}_\nu. \tag{16}$$

Equation (16) follows from the hypothesis that the distortions associated with remodelling obey an evolution law of the same type as the normality rule of isotropic, associative, finite-strain plasticity. For this reason, the physical quantity that represents them, i.e., $\tilde{\boldsymbol{D}}_\mathrm{p}$, has to be co-directional with $\tilde{\boldsymbol{\Sigma}}_\nu$ (see Sections 95.5 and 98 of Gurtin et al.[43]). In turn, this condition is automatically satisfied by introducing the direction tensor $\boldsymbol{N}_\nu$ and requiring $\tilde{\boldsymbol{D}}_\mathrm{p}$ to be proportional to $\boldsymbol{N}_\nu$. Clearly, this identifies the corresponding proportionality factor with the norm of $\tilde{\boldsymbol{D}}_\mathrm{p}$.

In (15) and (16), the norms $\|\tilde{\boldsymbol{\Sigma}}_\nu\|_{\boldsymbol{\eta}}$ and $\|\tilde{\boldsymbol{D}}_\mathrm{p}\|_{\boldsymbol{\eta}^{-1}}$ are defined by

$$\|\tilde{\boldsymbol{\Sigma}}_\nu\|_{\boldsymbol{\eta}} = \sqrt{\mathrm{tr}\left[\left(\boldsymbol{\eta}\tilde{\boldsymbol{\Sigma}}_\nu\boldsymbol{\eta}\right)^\mathrm{T}\tilde{\boldsymbol{\Sigma}}_\nu\right]}, \tag{17a}$$

$$\|\tilde{\boldsymbol{D}}_\mathrm{p}\|_{\boldsymbol{\eta}^{-1}} = \sqrt{\mathrm{tr}\left[\boldsymbol{\eta}^{-1}\tilde{\boldsymbol{D}}_\mathrm{p}\boldsymbol{\eta}^{-1}\tilde{\boldsymbol{D}}_\mathrm{p}\right]}, \tag{17b}$$

and their product coincides with the double contraction $\tilde{\boldsymbol{\Sigma}}_\nu : \tilde{\boldsymbol{D}}_\mathrm{p} = \|\tilde{\boldsymbol{\Sigma}}_\nu\|_{\boldsymbol{\eta}}\|\tilde{\boldsymbol{D}}_\mathrm{p}\|_{\boldsymbol{\eta}^{-1}}$. Moreover, to simplify the notation, we invoke the definition of *accumulated plastic strain*[22,44], ε_p, i.e.,

$$\varepsilon_\mathrm{p}(X,t) \equiv \sqrt{\tfrac{2}{3}}\int_0^t \|\tilde{\boldsymbol{D}}_\mathrm{p}(X,\tau)\|_{\boldsymbol{\eta}^{-1}}\mathrm{d}\tau \quad \Rightarrow \quad \dot{\varepsilon}_\mathrm{p}(X,t) = \sqrt{\tfrac{2}{3}}\,\|\tilde{\boldsymbol{D}}_\mathrm{p}(X,t)\|_{\boldsymbol{\eta}^{-1}}, \tag{18}$$

so that Equation (16) becomes

$$\tilde{\boldsymbol{D}}_\mathrm{p} = \sqrt{\tfrac{3}{2}}\,\dot{\varepsilon}_\mathrm{p}\boldsymbol{N}_\nu. \tag{19}$$

Finally, by substituting (19) into (14), we obtain

$$\dot{\boldsymbol{F}}_\mathrm{p} = \left(\sqrt{\tfrac{3}{2}}\,\dot{\varepsilon}_\mathrm{p}\boldsymbol{\eta}^{-1}\boldsymbol{N}_\nu\right)\boldsymbol{F}_\mathrm{p} \quad \Rightarrow \quad \boldsymbol{L}_\mathrm{p} = \sqrt{\tfrac{3}{2}}\,\dot{\varepsilon}_\mathrm{p}\boldsymbol{\eta}^{-1}\boldsymbol{N}_\nu. \tag{20}$$

Equation (20) implies that, once $\boldsymbol{N}_\nu$ is assigned, $\boldsymbol{L}_\mathrm{p}$ has only one independent coefficient, given by $\dot{\varepsilon}_\mathrm{p}$. The important consequence of this result is that the body's structural degrees of freedom, originally represented by the tensorial quantity $\boldsymbol{F}_\mathrm{p}$, condense into the scalar variable ε_p.

Remark 1. Descriptive adequacy of ε_p. According to Equation (18), $\varepsilon_\mathrm{p}(X,t)$ is well-defined for all the tensor fields $\tilde{\boldsymbol{D}}_\mathrm{p}$ such that the norm $\|\tilde{\boldsymbol{D}}_\mathrm{p}(X,\,\cdot\,)\|_{\boldsymbol{\eta}^{-1}}$ is an integrable function of time over $[0,t]$, for every $X \in \mathscr{B}$ and $t \in [0,+\infty[$. Coherently with this definition, $\varepsilon_\mathrm{p}(X,t)$ keeps track of all the magnitudes of the rates of inelastic distortions, $\tilde{\boldsymbol{D}}_\mathrm{p}(X,\tau)$, which have occurred in a given material over $[0,t]$. For this reason, ε_p is a suitable descriptor of the mechanical response of materials that are capable of "perfectly memorising" inelastic distortions, as is the case for metals exhibiting rate-independent plasticity[67]. Biological

tissues, on the contrary, are often modelled as viscoelastic materials [7,8], and show fading memory effects. Nonetheless, as discussed in the Introduction, the experiments on cellular aggregates reported in [8,38] seem to suggest the existence of inelastic distortions that do not fade away in time, unless some active process restores the original configuration of the aggregates. For these reasons, $\varepsilon_{\rm p}$ can be regarded as appropriate for describing the inelastic distortions accumulated in a tissue from the beginning of its loading history. Should the active processes be considered, they could be accounted for by introducing another factor, denoted e.g. by $\boldsymbol{F}_{\rm a}$, and representing the active part of the tissue's deformation [68].

We switch now to the constraints placed on $\boldsymbol{F}_\gamma$, and we analyse their impact on the way in which the mass balance law (8b) can be reformulated. Upon using the decomposition $J = J_{\rm e}J_{\rm p}J_\gamma$, and recalling the condition $J_{\rm p} = 1$, we rewrite $\Phi_{\rm s}$ as $\Phi_{\rm s} = J_\gamma \Phi_{{\rm s}\nu}$, where $\Phi_{{\rm s}\nu}$ is such that $\Phi_{{\rm s}\nu}(X,t) = J_{\rm e}(X,t)\varphi_{\rm s}(\chi(X,t),t)$, and indicates, thus, the solid phase volumetric fraction with respect to the volume measure of the *natural state*. Hence, Equation (8b) becomes

$$\rho_{{\rm s}0}\dot{J}_\gamma \Phi_{{\rm s}\nu} + \rho_{{\rm s}0} J_\gamma \dot{\Phi}_{{\rm s}\nu} = R_{\rm s}. \tag{21}$$

A rather standard hypothesis in the mechanics of growth, see e.g. [27,28,53,69], is to choose $\boldsymbol{F}_\gamma$ in such a way that the time derivative of its determinant, $\dot{J}_\gamma$, compensates for the mass source $R_{\rm s}$. In other words, by exploiting the identity $\dot{J}_\gamma = J_\gamma {\rm tr}[\dot{\boldsymbol{F}}_\gamma \boldsymbol{F}_\gamma^{-1}] = J_\gamma {\rm tr}[\boldsymbol{L}_\gamma]$, we require the fulfilment of the auxiliary condition

$$\rho_{{\rm s}0} J_\gamma \Phi_{{\rm s}\nu} {\rm tr}[\boldsymbol{L}_\gamma] = R_{\rm s} \quad \Rightarrow \quad {\rm tr}[\boldsymbol{L}_\gamma] = \frac{R_{\rm s}}{\rho_{{\rm s}0}\Phi_{{\rm s}\nu} J_\gamma}, \tag{22}$$

which constitutes the *first constraint* on $\boldsymbol{F}_\gamma$. Such constraint has, in fact, non-holonomic nature, since it is defined through a non-homogeneous algebraic condition on the generalised (tensorial) velocity $\boldsymbol{L}_\gamma$. Plugging (22) into (21) yields $\rho_{{\rm s}0} J_\gamma \dot{\Phi}_{{\rm s}\nu} = 0$, thereby implying that the volumetric fraction $\Phi_{{\rm s}\nu}$ is necessarily independent of time.

The *second constraint* on $\boldsymbol{F}_\gamma$ is provided by the phenomenological evidence according to which, for the class of problems under study, growth occurs isotropically [4]. The consequences of this fact on the admissible choices of the growth tensor can be deduced by looking at the polar decompositions of $\boldsymbol{F}_\gamma$. Indeed, by considering for instance the right decomposition, $\boldsymbol{F}_\gamma = \boldsymbol{\mathcal{R}}_\gamma \boldsymbol{U}_\gamma$, where $\boldsymbol{\mathcal{R}}_\gamma$ is the rotation tensor and $\boldsymbol{U}_\gamma$ is the stretch tensor associated with $\boldsymbol{F}_\gamma$, the isotropy of growth translates to the kinematic restrictions $\boldsymbol{\mathcal{R}}_\gamma = \boldsymbol{I}$ and $\boldsymbol{U}_\gamma = \gamma \boldsymbol{I}$, where $\boldsymbol{I}$ is the identity tensor. Therefore, it holds that $\boldsymbol{F}_\gamma = \gamma \boldsymbol{I}$ and (22) can be rephrased as

$$\frac{\dot{\gamma}}{\gamma} = \frac{R_{\rm s}}{3\rho_{{\rm s}0}\Phi_{{\rm s}\nu} J_\gamma} \quad \Rightarrow \quad \dot{\gamma} = \frac{R_{\rm s}}{3\rho_{{\rm s}0}\Phi_{{\rm s}\nu}\gamma^2}. \tag{23}$$

Finally, we notice that Equation (8d) can be regarded as a constraint on the material filtration velocity, $\boldsymbol{Q}$, expressed through a restriction on its divergence.

3 | PRINCIPLE OF VIRTUAL POWERS

After laying down the kinematic picture that describes the problem under investigation, we select the generalised velocities upon which the system's mechanical power is defined. Summarising the discussion reported above, such velocities may be enlisted in the following collection of fields

$$\mathcal{V} = (\boldsymbol{v}_{\rm s}, \nabla \boldsymbol{v}_{\rm s}, {\rm D_s}\varepsilon_{\rm p}, {\rm D_s e_p}, \nabla\big({\rm D_s e_p}\big) \mid \boldsymbol{v}_{\rm f}, \nabla \boldsymbol{v}_{\rm f}), \tag{24}$$

which will be employed to define the internal and the external mechanical powers. We remark that, whereas the fluid phase requires only $\boldsymbol{v}_{\rm f}$ and $\nabla \boldsymbol{v}_{\rm f}$ for the characterisation of the system's internal power, the solid phase necessitates both *standard* and *non-standard* descriptors. The standard ones, i.e., $\boldsymbol{v}_{\rm s}$ and $\nabla \boldsymbol{v}_{\rm s}$, account only for the *"visible"* changes of shape of the system (here, the word *"visible"* is meant in the sense of DiCarlo and Quiligotti [29]), while the non-standard terms are the generalised velocities ${\rm D_s}\varepsilon_{\rm p}$, ${\rm D_s e_p}$, and $\nabla({\rm D_s e_p})$, introduced to define the power expended to accomplish the structural changes of the system. As anticipated in the Introduction, the main motivation for taking the approach of Anand et al. [44] and specialising it to our problem is that it allows to develop a strain-gradient formulation of remodelling based on the scalar variable ${\rm e_p}$. The latter is defined as the micro-scale counterpart of the accumulated remodelling strain, $\varepsilon_{\rm p}$, and, as such, it is assumed to "condense" in itself all the information about the inelastic processes that determine the micro-scale remodelling of the tissue under study. Moreover, since it is an "effective" representative of these processes, it prevents from the introduction of a micro-scale, second-order remodelling tensor, which would render the theoretical and numerical analysis of the problem at hand much more complicated. Accordingly, the generalised velocities associated with ${\rm e_p}$, i.e., ${\rm D_s e_p}$ and $\nabla({\rm D_s e_p})$, are a scalar and a co-vector field, rather than

being a second-order and a third-order tensor field, respectively. It follows from these considerations that an inelastic model built on ε_{p} and e_{p} has the right to stand on its own, independently on any numerical issue, even though Anand et al.[44] have originally introduced e_{p} for numerical purposes. Clearly, such a model represents the limit case of more elaborated theories that involve tensor fields, rather than scalar ones.

Coherently with (24), we introduce the collection of virtual velocities

$$\mathcal{V}_{\mathrm{v}} = (\boldsymbol{u}_{\mathrm{s}}, \nabla \boldsymbol{u}_{\mathrm{s}}, u_{\varepsilon}, u_{\mathrm{p}}, \nabla u_{\mathrm{p}} | \, \boldsymbol{u}_{\mathrm{f}}, \nabla \boldsymbol{u}_{\mathrm{f}}) \in \mathscr{V}_{\mathrm{v}}, \tag{25}$$

where $\mathscr{V}_{\mathrm{v}}$ is referred to as the set of all virtual velocities. The elements $\boldsymbol{u}_{\mathrm{s}}$, $\nabla \boldsymbol{u}_{\mathrm{s}}$, $\boldsymbol{u}_{\mathrm{f}}$, and $\nabla \boldsymbol{u}_{\mathrm{f}}$ are the virtual counterparts of $\boldsymbol{v}_{\mathrm{s}}$, $\nabla \boldsymbol{v}_{\mathrm{s}}$, $\boldsymbol{v}_{\mathrm{f}}$, and $\nabla \boldsymbol{v}_{\mathrm{f}}$, respectively, and the non-standard fields u_{ε}, u_{p}, and ∇u_{p} denote the virtual velocities corresponding to the rates $\mathrm{D_s}\varepsilon_{\mathrm{p}}$, $\mathrm{D_s e_p}$, and $\nabla(\mathrm{D_s e_p})$, respectively.

Once the virtual velocities of the model are identified, it is possible to write the internal and the external virtual powers of the system. These two linear and continuous functionals are defined over $\mathscr{V}_{\mathrm{v}}$, and are specified through the expressions

$$\mathcal{W}_{\mathrm{v}}^{(\mathrm{i})}(\mathcal{V}_{\mathrm{v}}) \equiv \int_{\mathscr{C}_t} \left\{ \boldsymbol{\sigma}_{\mathrm{s}} : \boldsymbol{g} \nabla \boldsymbol{u}_{\mathrm{s}} + \boldsymbol{m}_{\mathrm{s}} . \boldsymbol{u}_{\mathrm{s}} + \boldsymbol{\sigma}_{\mathrm{f}} : \boldsymbol{g} \nabla \boldsymbol{u}_{\mathrm{f}} + \boldsymbol{m}_{\mathrm{f}} . \boldsymbol{u}_{\mathrm{f}} + h_{\varepsilon}^{(\mathrm{i})} u_{\varepsilon} + h_{\mathrm{p}}^{(\mathrm{i})} u_{\mathrm{p}} + \boldsymbol{\xi}_{\mathrm{p}} \nabla u_{\mathrm{p}} \right\}, \tag{26a}$$

$$\mathcal{W}_{\mathrm{v}}^{(\mathrm{e})}(\mathcal{V}_{\mathrm{v}}) \equiv \int_{\Gamma_t^N} \left\{ \boldsymbol{\tau}_{\mathrm{s}} . \boldsymbol{u}_{\mathrm{s}} + \boldsymbol{\tau}_{\mathrm{f}} . \boldsymbol{u}_{\mathrm{f}} + \zeta_{\mathrm{p}} u_{\mathrm{p}} \right\} + \int_{\mathscr{C}_t} \left\{ h_{\varepsilon}^{(\mathrm{e})} u_{\varepsilon} + h_{\mathrm{p}}^{(\mathrm{e})} u_{\mathrm{p}} \right\}, \tag{26b}$$

respectively. Here, $\mathscr{C}_t \subset \mathcal{S}$ is the portion of the Euclidean space in which the solid and the fluid phase co-exist, and $\Gamma_t^N \subset \partial \mathscr{C}_t$ is the portion of the boundary of $\mathscr{C}_t$ on which Neumann conditions are imposed. In (26a), $\boldsymbol{\sigma}_{\mathrm{s}}$ and $\boldsymbol{\sigma}_{\mathrm{f}}$ are the Cauchy stress tensors of the solid and of the fluid, $\boldsymbol{m}_{\mathrm{s}}$ and $\boldsymbol{m}_{\mathrm{f}}$ are internal forces that describe the gain or loss of momentum of the solid and of the fluid in response to exchange interactions between the two phases, $h_{\varepsilon}^{(\mathrm{i})}$ and $h_{\mathrm{p}}^{(\mathrm{i})}$ are internal generalised forces dual to u_{ε} and u_{p}, respectively, and $\boldsymbol{\xi}_{\mathrm{p}}$ is the generalised stress-like field dual to ∇u_{p}. We notice that, since the virtual velocities u_{ε} and u_{p} are scalar fields, the forces dual to them must be representable by scalars. Following the same logic, supplied by duality, since ∇u_{p} is a co-vector by definition, its power-conjugate force, $\boldsymbol{\xi}_{\mathrm{p}}$, must be a vector-like field. On the same footing, in addition to the standard vector-like contact forces $\boldsymbol{\tau}_{\mathrm{s}}$ and $\boldsymbol{\tau}_{\mathrm{f}}$, in (26b) we introduce the contact force ζ_{p} and the "bulk" external forces $h_{\varepsilon}^{(\mathrm{e})}$ and $h_{\mathrm{p}}^{(\mathrm{e})}$, all being scalar-like for the reasons explained above.

By requiring the internal virtual power, $\mathcal{W}_{\mathrm{v}}^{(\mathrm{i})}(\mathcal{V}_{\mathrm{v}})$, to be invariant under the superposition of arbitrary rigid motions, we deduce the symmetry of the total stress tensor, $\boldsymbol{\sigma} = \boldsymbol{\sigma}_{\mathrm{s}} + \boldsymbol{\sigma}_{\mathrm{f}}$, and that the sum of the internal forces $\boldsymbol{m}_{\mathrm{s}}$ and $\boldsymbol{m}_{\mathrm{f}}$ must vanish identically, i.e., we obtain the condition $\boldsymbol{m}_{\mathrm{s}} + \boldsymbol{m}_{\mathrm{f}} = \boldsymbol{0}$[58]. Consistently with the *a priori* exclusion of all inertial terms from our model, this last result constitutes an approximation of the more general balance of internal forces that, for a biphasic medium with mass exchange between the phases, is given by $\boldsymbol{m}_{\mathrm{s}} + r_{\mathrm{s}} \boldsymbol{v}_{\mathrm{s}} + \boldsymbol{m}_{\mathrm{f}} - r_{\mathrm{s}} \boldsymbol{v}_{\mathrm{f}} = \boldsymbol{0}$. In fact, the approximation consists of dropping the term $r_{\mathrm{s}} \boldsymbol{v}_{\mathrm{s}} - r_{\mathrm{s}} \boldsymbol{v}_{\mathrm{f}} = -r_{\mathrm{s}} \boldsymbol{w}$, and is based on the argument that the interphase mass transfer, r_{s}, depends on the micro-scale velocity with which the mass passes from the fluid to the solid, and vice versa. Such velocity, multiplied by the relative macro-scale velocity $\boldsymbol{w}$, is assumed to produce a rate of momentum exchange that weighs much less than $\boldsymbol{m}_{\mathrm{s}}$ and $\boldsymbol{m}_{\mathrm{f}}$, thereby leading to the desired approximation.

We emphasise that, in writing the expressions of $\mathcal{W}_{\mathrm{v}}^{(\mathrm{i})}(\mathcal{V}_{\mathrm{v}})$ and $\mathcal{W}_{\mathrm{v}}^{(\mathrm{e})}(\mathcal{V}_{\mathrm{v}})$, we have omitted *all* inertial and long-range (e.g. gravity) forces, which we regard as negligible from the outset. Moreover, the nature of the forces $h_{\mathrm{p}}^{(\mathrm{i})}$ and $\boldsymbol{\xi}_{\mathrm{p}}$ is necessarily coherent with the hypothesis that the kinematics of the solid phase micro-structure is represented by e_{p} and $\nabla \mathrm{e}_{\mathrm{p}}$. In this sense, the model features some important similarities with Gurtin's approach to the derivation of the generalised Allen-Cahn equation[52], in which the scalar field describing the micro-structural kinematics of the considered medium is regarded as an order parameter.

Looking at (26a) and (26b), we also notice that, in principle, also the velocity and the velocity gradient of the nutrients should be considered, along with their virtual counterparts, in (24) and (25). However, in view of a comprehensive formulation of the Principle of Virtual Powers, this would call for the definition of the generalised forces expending power on them, and, above all, for the introduction of surface tractions, acting on Γ_t^N. Individuating a physically sound way for expressing such contact forces is not easy and taking them into account leads unavoidably to both theoretical and computational complications (see, e.g., Grillo et al.[36] for an attempt of including these forces, based on a work by Sciarra et al.[70]). For these reasons, we present here a simplified framework in which we account for the nutrients through the balance law (3a), while we omit to study their kinematics and dynamics in detail. In other words, due to their tantamount importance for activating growth, we do include them in our model, but we do not treat them systematically. Hence, we do not consider any force balance associated with the nutrients, nor do we investigate their contribution to the dissipation inequality (see Section 4). Rather, with reference

to (3a), we "guess" that the mass flux vector, $\boldsymbol{y}_{\mathrm{N}}$, obeys a diffusion dynamics of Fickean type, so that it is prescribed to have the form $\boldsymbol{y}_{\mathrm{N}} = -\rho_{\mathrm{f}0}\boldsymbol{d}\nabla c_{\mathrm{N}}$ in the Eulerian description and $\boldsymbol{Y}_{\mathrm{N}} = -\rho_{\mathrm{f}0}\boldsymbol{D}\,\mathrm{Grad}\,\omega_{\mathrm{N}}$ in material formalism, with $\boldsymbol{d}$ being the diffusivity tensor and $\boldsymbol{D}$ its material counterpart. Note that the latter is related to $\boldsymbol{d}$ through the backward Piola transformation $\boldsymbol{D}(X,t) = \boldsymbol{J}(X,t)\boldsymbol{F}^{-1}(\chi(X,t),t)\boldsymbol{d}(\chi(X,t),t)\boldsymbol{F}^{-\mathrm{T}}(X,t)$.

By invoking the Principle of Virtual Powers, we enforce the condition $\mathcal{W}_{\mathrm{v}}^{(\mathrm{i})}(\mathcal{V}_{\mathrm{v}}) = \mathcal{W}_{\mathrm{v}}^{(\mathrm{e})}(\mathcal{V}_{\mathrm{v}})$, which is required to be fulfilled for any admissible set of generalised velocities $\mathcal{V}_{\mathrm{v}}$, thereby leading to

$$\int_{\mathscr{C}_t} \Big\{ \big[-\mathrm{div}\boldsymbol{\sigma}_{\mathrm{s}} + \boldsymbol{m}_{\mathrm{s}}\big].\boldsymbol{u}_{\mathrm{s}} + \big[-\mathrm{div}\boldsymbol{\sigma}_{\mathrm{f}} + \boldsymbol{m}_{\mathrm{f}}\big].\boldsymbol{u}_{\mathrm{f}} + [h_{\varepsilon}^{(\mathrm{i})} - h_{\varepsilon}^{(\mathrm{e})}]u_{\varepsilon} + [h_{\mathrm{p}}^{(\mathrm{i})} - \mathrm{div}\boldsymbol{\xi}_{\mathrm{p}} - h_{\mathrm{p}}^{(\mathrm{e})}]u_{\mathrm{p}} \Big\}$$
$$+ \int_{\Gamma_t^N} \big\{ [\boldsymbol{\sigma}_{\mathrm{s}}.\boldsymbol{n} - \boldsymbol{\tau}_{\mathrm{s}}].\boldsymbol{u}_{\mathrm{s}} + [\boldsymbol{\sigma}_{\mathrm{f}}.\boldsymbol{n} - \boldsymbol{\tau}_{\mathrm{f}}].\boldsymbol{u}_{\mathrm{f}} + [\boldsymbol{\xi}_{\mathrm{p}}.\boldsymbol{n} - \zeta_{\mathrm{p}}]u_{\mathrm{p}} \big\} = 0. \tag{27}$$

By adopting the usual localisation procedure that extracts the local form of the equations of motion from the Principle of Virtual Powers, Equation (27) yields the following balances of generalised forces

$$\boldsymbol{m}_{\mathrm{s}} - \mathrm{div}\boldsymbol{\sigma}_{\mathrm{s}} = \boldsymbol{0}, \tag{28a}$$
$$\boldsymbol{m}_{\mathrm{f}} - \mathrm{div}\boldsymbol{\sigma}_{\mathrm{f}} = \boldsymbol{0}, \tag{28b}$$
$$h_{\varepsilon}^{(\mathrm{i})} - h_{\varepsilon}^{(\mathrm{e})} = 0, \tag{28c}$$
$$h_{\mathrm{p}}^{(\mathrm{i})} - \mathrm{div}\boldsymbol{\xi}_{\mathrm{p}} - h_{\mathrm{p}}^{(\mathrm{e})} = 0, \tag{28d}$$

which hold in $\mathscr{C}_t$, and the balances of contact forces on Γ_t^N

$$\boldsymbol{\sigma}_{\mathrm{s}}.\boldsymbol{n} - \boldsymbol{\tau}_{\mathrm{s}} = \boldsymbol{0}, \tag{29a}$$
$$\boldsymbol{\sigma}_{\mathrm{f}}.\boldsymbol{n} - \boldsymbol{\tau}_{\mathrm{f}} = \boldsymbol{0}, \tag{29b}$$
$$\boldsymbol{\xi}_{\mathrm{p}}.\boldsymbol{n} - \zeta_{\mathrm{p}} = 0. \tag{29c}$$

It is worthwhile to mention that, in general, upon defining the field of *total* contact forces $\boldsymbol{\tau} = \boldsymbol{\tau}_{\mathrm{s}} + \boldsymbol{\tau}_{\mathrm{f}}$, and the *total* Cauchy stress tensor $\boldsymbol{\sigma} = \boldsymbol{\sigma}_{\mathrm{s}} + \boldsymbol{\sigma}_{\mathrm{f}}$, it is rather natural to provide on Γ_t^N boundary conditions of the kind $\boldsymbol{\sigma}.\boldsymbol{n} = \boldsymbol{\tau}$ (see[70] for details). Nevertheless, even in that case, the boundary conditions (29a) and (29b) can be recovered under the assumption that $\boldsymbol{\tau}_{\mathrm{s}}$ and $\boldsymbol{\tau}_{\mathrm{f}}$ are obtained by partitioning $\boldsymbol{\tau}$ as $\boldsymbol{\tau}_{\mathrm{s}} = (\rho_{\mathrm{s}0}\varphi_{\mathrm{s}}/\rho)\boldsymbol{\tau}$ and $\boldsymbol{\tau}_{\mathrm{f}} = (\rho_{\mathrm{f}0}\varphi_{\mathrm{f}}/\rho)\boldsymbol{\tau}$, respectively.

4 | DISSIPATION AND DYNAMIC EQUATIONS

To extract constitutive information on the internal forces presented so far, we study the dissipation inequality of the system. For this purpose, we enrich the picture proposed in Grillo et al.[36], which, in turn, was inspired by Hassanizadeh[71] and Benethum et al.[72]. This is done by framing the formulation of Anand et al.[44] in the context of biphasic media and, above all, by rephrasing it in order to account for growth. The first step in this direction is to introduce the dissipation density, $\mathcal{D}$, measured per unit volume of the current configuration of the medium, and defining the dissipation associated with an open subset $\Omega_t \subset \mathscr{C}_t$ as

$$\int_{\Omega_t} \mathcal{D} = -\int_{\Omega_t} \big\{ r_{\mathrm{s}}(\psi_{\mathrm{s}} - \psi_{\mathrm{f}}) + \rho_{\mathrm{s}0}\varphi_{\mathrm{s}}\mathrm{D}_{\mathrm{s}}\psi_{\mathrm{s}} + \rho_{\mathrm{f}0}\varphi_{\mathrm{f}}\mathrm{D}_{\mathrm{s}}\psi_{\mathrm{f}} + (\rho_{\mathrm{f}0}\varphi_{\mathrm{f}}\nabla\psi_{\mathrm{f}})\boldsymbol{w} \big\}$$
$$+ \int_{\partial\Omega_t} \big\{ (\boldsymbol{\sigma}_{\mathrm{s}}.\boldsymbol{n}).\boldsymbol{v}_{\mathrm{s}} + (\boldsymbol{\sigma}_{\mathrm{f}}.\boldsymbol{n}).\boldsymbol{v}_{\mathrm{f}} + (\boldsymbol{\xi}_{\mathrm{p}}.\boldsymbol{n})\mathrm{D}_{\mathrm{s}}\mathrm{e}_{\mathrm{p}} \big\} + \int_{\Omega_t} \Big\{ h_{\varepsilon}^{(\mathrm{e})}\mathrm{D}_{\mathrm{s}}\varepsilon_{\mathrm{p}} + h_{\mathrm{p}}^{(\mathrm{e})}\mathrm{D}_{\mathrm{s}}\mathrm{e}_{\mathrm{p}} \Big\} + \int_{\Omega_t} \mathcal{D}_{\gamma} \geq 0. \tag{30}$$

As shown in (30), the dissipation can be written as the sum of four different contributions: with reference to the first integral of the sum defining $\int_{\Omega_t}\mathcal{D}$, we recognise that, by indicating with ψ_{s} and ψ_{f} the Helmholtz free energies per unit mass of the solid and of the fluid, the term $r_{\mathrm{s}}(\psi_{\mathrm{s}} - \psi_{\mathrm{f}})$ expresses the rate of change of the free energy densities, $\rho_{\mathrm{s}0}\varphi_{\mathrm{s}}\psi_{\mathrm{s}}$ and $\rho_{\mathrm{f}0}\varphi_{\mathrm{f}}\psi_{\mathrm{f}}$, due to the mass exchange between the phases. Moreover, $\rho_{\mathrm{s}0}\varphi_{\mathrm{s}}\mathrm{D}_{\mathrm{s}}\psi_{\mathrm{s}}$ and $\rho_{\mathrm{f}0}\varphi_{\mathrm{f}}\mathrm{D}_{\mathrm{s}}\psi_{\mathrm{f}}$ are the rates of change of the Helmholtz free energy densities measured with respect to the solid phase motion, and $(\nabla\psi_{\mathrm{f}})\boldsymbol{w}$ describes how ψ_{f} is transported due to the motion of the fluid relative to the solid. The terms in the surface integral denote the contributions to the net power expended on Ω_t due to the contact forces with the surrounding medium, while the terms in the third integral represent the part of net power ascribable

to the non-standard forces $h^{(e)}_{\varepsilon}$ and $h^{(e)}_{p}$. Finally, $\mathcal{D}_\gamma$ is a dissipation density introduced to account for the fact that the medium experiences growth (see e.g. [66] for a discussion on this issue).

By applying Gauss Theorem to the surface integral of Equation (30), and using the balance laws (28a)–(28d) and (29a)–(29c), the dissipation inequality becomes

$$\begin{aligned}\int_{\Omega_t} \mathcal{D} = &-\int_{\Omega_t} \left\{ r_s(\psi_s - \psi_f) + \rho_{s0}\varphi_s \mathrm{D}_s\psi_s + \rho_{f0}\varphi_f \mathrm{D}_s\psi_f + (\rho_{f0}\varphi_f \nabla\psi_f)\boldsymbol{w} \right\} \\ &+ \int_{\Omega_t} \left\{ \boldsymbol{m}_s.\boldsymbol{v}_s + \boldsymbol{\sigma}_s : \boldsymbol{g}\nabla\boldsymbol{v}_s + \boldsymbol{m}_f.\boldsymbol{v}_f + \boldsymbol{\sigma}_f : \boldsymbol{g}\nabla\boldsymbol{v}_f + h^{(i)}_p \mathrm{D}_s e_p + \boldsymbol{\xi}_p \nabla(\mathrm{D}_s e_p) + h^{(i)}_{\varepsilon} \mathrm{D}_s\varepsilon_p \right\} + \int_{\Omega_t} \mathcal{D}_\gamma \geq 0. \end{aligned} \tag{31}$$

By localising Equation (31) and invoking the condition $\boldsymbol{m}_s + \boldsymbol{m}_f = \boldsymbol{0}$, we obtain

$$\begin{aligned}\mathcal{D} = &\, r_s(\psi_f - \psi_s) - \rho_{s0}\varphi_s \mathrm{D}_s\psi_s - \rho_{f0}\varphi_f \mathrm{D}_s\psi_f + [\boldsymbol{m}_f - \boldsymbol{g}^{-1}(\rho_{f0}\varphi_f \nabla\psi_f)].\boldsymbol{w} \\ &+ \boldsymbol{\sigma}_s : \boldsymbol{g}\nabla\boldsymbol{v}_s + \boldsymbol{\sigma}_f : \boldsymbol{g}\nabla\boldsymbol{v}_f + h^{(i)}_p \mathrm{D}_s e_p + \boldsymbol{\xi}_p \nabla(\mathrm{D}_s e_p) + h^{(i)}_{\varepsilon} \mathrm{D}_s\varepsilon_p + \mathcal{D}_\gamma \geq 0. \end{aligned} \tag{32}$$

As a simplifying assumption, we approximate the Helmholtz free energy density of the fluid, ψ_f, with a constant, so that $\rho_{f0}\varphi_f \mathrm{D}_s\psi_f$ and $\nabla\psi_f$ are negligible with respect to all the other terms featuring in the dissipation inequality. Such situation occurs, for instance, when the state variables characterising ψ_f are, at the most, the temperature and the mass fraction of the nutrients dissolved in the fluid, and the latter is so low that ψ_f can be safely set equal to the (constant) Helmholtz free energy density of water at constant temperature. Under these hypotheses, Equation (32) becomes

$$\mathcal{D} = r_s(\psi_f - \psi_s) - \rho_{s0}\varphi_s \mathrm{D}_s\psi_s + \boldsymbol{m}_f.\boldsymbol{w} + \boldsymbol{\sigma}_s : \boldsymbol{g}\nabla\boldsymbol{v}_s + \boldsymbol{\sigma}_f : \boldsymbol{g}\nabla\boldsymbol{v}_f + h^{(i)}_p \mathrm{D}_s e_p + \boldsymbol{\xi}_p \nabla(\mathrm{D}_s e_p) + h^{(i)}_{\varepsilon} \mathrm{D}_s\varepsilon_p + \mathcal{D}_\gamma \geq 0. \tag{33}$$

It is convenient to rewrite the dissipation inequality per unit volume of $\mathscr{B}$. To do this, we perform a Piola transformation of (33), which yields

$$\mathcal{D}_R = R_s(\Psi_f - \Psi_s) - \rho_{s0} J_\gamma \Phi_{s\nu} \dot{\Psi}_s + \Phi_f^{-1} \boldsymbol{Q}\boldsymbol{M}_f + \boldsymbol{P}_s : \boldsymbol{g}\dot{\boldsymbol{F}} + \boldsymbol{P}_f : \boldsymbol{g}\mathrm{Grad}\boldsymbol{V}_f + H^{(i)}_p \dot{e}_p + \boldsymbol{\Xi}_p \mathrm{Grad}\dot{e}_p + H^{(i)}_{\varepsilon}\dot{\varepsilon}_p + J\mathcal{D}_\gamma \geq 0, \tag{34}$$

where, as anticipated above, $R_s(X,t) = J(X,t) r_s(\chi(X,t),t)$ is the material form of the source/sink of mass for the solid phase as a whole, and we introduced the notation

$$\Psi_\alpha(X,t) = \psi_\alpha(\chi(X,t),t), \qquad \alpha \in \{f,s\}, \tag{35a}$$

$$\boldsymbol{P}_\alpha(X,t) = J(X,t)\boldsymbol{\sigma}_\alpha(\chi(X,t),t)\boldsymbol{F}^{-T}(X,t), \qquad \alpha \in \{f,s\}, \tag{35b}$$

$$H^{(i)}_\beta(X,t) = J(X,t) h^{(i)}_\beta(\chi(X,t),t), \qquad \beta \in \{p,\varepsilon\}, \tag{35c}$$

$$\boldsymbol{\Xi}_p(X,t) = J(X,t)\boldsymbol{\xi}_p(\chi(X,t),t)\boldsymbol{F}^{-T}(X,t), \tag{35d}$$

$$\boldsymbol{M}_f(X,t) = J(X,t)[\boldsymbol{g}(\chi(X,t))\boldsymbol{m}_f(\chi(X,t),t)]\boldsymbol{F}(X,t). \tag{35e}$$

Here, $\boldsymbol{P}_f$ and $\boldsymbol{P}_s$ indicate the first Piola-Kirchhoff stress tensors of the fluid and the solid phase, $H^{(i)}_p$ and $H^{(i)}_{\varepsilon}$ express, in material form, the internal generalised forces dual to $\dot{e}_p$ and $\dot{\varepsilon}_p$, respectively, $\boldsymbol{\Xi}_p$ is the material representation of the stress-like generalised force, $\boldsymbol{\xi}_p$, and is thus dual to $\mathrm{Grad}\dot{e}_p$, and $\boldsymbol{M}_f$, re-defined as a covector, is the material counterpart of the momentum exchange rate $\boldsymbol{m}_f$.

Finally, by generalising the Helmholtz free energy density proposed by [44], we prescribe Ψ_s to be given by the sum of three terms, i.e.,

$$\hat{\Psi}_s(\boldsymbol{F},\boldsymbol{F}_p,\boldsymbol{F}_\gamma,\varepsilon_p,e_p,\mathrm{Grad}e_p) = \hat{\Psi}^{(st)}_s(\boldsymbol{F}\boldsymbol{F}_\gamma^{-1}\boldsymbol{F}_p^{-1}) + \tfrac{1}{2}a_0[\varepsilon_p - e_p]^2 + \tfrac{1}{2}b_0\boldsymbol{F}_\gamma^{-1}\boldsymbol{B}_p\boldsymbol{F}_\gamma^{-T} : \mathrm{Grad}e_p \otimes \mathrm{Grad}e_p, \tag{36}$$

with $\boldsymbol{B}_p = \boldsymbol{F}_p^{-1}.\boldsymbol{F}_p^{-T}$, so that the time derivative of Ψ_s reads

$$\begin{aligned}\dot{\Psi}_s = &\left(\frac{\partial\hat{\Psi}^{(st)}_s}{\partial\boldsymbol{F}_e}\boldsymbol{F}_p^{-T}\boldsymbol{F}_\gamma^{-T} \right) : \dot{\boldsymbol{F}} - \frac{1}{3}\frac{\mathrm{tr}(\boldsymbol{\eta}\boldsymbol{\Sigma}_\nu)}{\rho_{s0}\Phi_{s\nu}}\frac{R_s}{\rho_{s0}\Phi_{s\nu}J_\gamma} - \frac{1}{\rho_{s0}\Phi_{s\nu}}\left\{ \sqrt{\tfrac{3}{2}}\|\tilde{\boldsymbol{\Sigma}}_\nu\|_{\boldsymbol{\eta}} - A_\nu[\varepsilon_p - e_p] \right\}\dot{\varepsilon}_p \\ &- \frac{A_\nu}{\rho_{s0}\Phi_{s\nu}}[\varepsilon_p - e_p]\dot{e}_p + \frac{B_\nu}{\rho_{s0}\Phi_{s\nu}}\left[\left(\boldsymbol{F}_\gamma^{-1}\boldsymbol{B}_p\boldsymbol{F}_\gamma^{-T}\right)\mathrm{Grad}e_p \right]\overline{\mathrm{Grad}e_p}, \end{aligned} \tag{37}$$

where $\hat{\Psi}^{(st)}_s$ is differentiated with respect to $\boldsymbol{F}_e = \boldsymbol{F}\boldsymbol{F}_\gamma^{-1}\boldsymbol{F}_p^{-1}$. In (37), we introduced the notation

$$\boldsymbol{\Sigma}_\nu = \boldsymbol{\eta}^{-1}\boldsymbol{F}_e^T\left(\rho_{s0}\Phi_{s\nu}\frac{\partial\hat{\Psi}^{(st)}_s}{\partial\boldsymbol{F}_e} \right) + B_\nu\left[\boldsymbol{\eta}^{-1}\boldsymbol{F}_p^{-T}\boldsymbol{F}_\gamma^{-T}\left(\mathrm{Grad}e_p \otimes \mathrm{Grad}e_p\right)\boldsymbol{F}_\gamma^{-1}\boldsymbol{F}_p^{-1}\boldsymbol{\eta}^{-1} \right], \tag{38a}$$

$$\tilde{\boldsymbol{\Sigma}}_\nu = \boldsymbol{\Sigma}_\nu - \tfrac{1}{3}\mathrm{tr}[\boldsymbol{\eta}\boldsymbol{\Sigma}_\nu]\boldsymbol{\eta}^{-1}, \tag{38b}$$

$$A_\nu = \rho_{\mathrm{s}0}\Phi_{\mathrm{s}\nu}a_0, \tag{38c}$$

$$B_\nu = \rho_{\mathrm{s}0}\Phi_{\mathrm{s}\nu}b_0, \tag{38d}$$

where A_ν and B_ν are the counterparts of the strictly positive constants a_0 and b_0, expressed per unit volume of the tissue's natural state, and $\boldsymbol{\Sigma}_\nu$ is a generalised Mandel stress tensor that comprises both the standard definition of the Mandel stress tensor, i.e.,

$$\boldsymbol{\Sigma}_\nu^{(\mathrm{st})} = \boldsymbol{\eta}^{-1}\boldsymbol{F}_{\mathrm{e}}^{\mathrm{T}}\left(\rho_{\mathrm{s}0}\Phi_{\mathrm{s}\nu}\frac{\partial\hat{\Psi}_{\mathrm{s}}^{(\mathrm{st})}}{\partial\boldsymbol{F}_{\mathrm{e}}}\right), \tag{39}$$

and the non-standard stress-like contribution

$$\boldsymbol{\Sigma}_\nu^{(\text{n-st})} = B_\nu\left[\boldsymbol{\eta}^{-1}\boldsymbol{F}_{\mathrm{p}}^{-\mathrm{T}}\boldsymbol{F}_\gamma^{-\mathrm{T}}\left(\mathrm{Grad}\mathfrak{e}_{\mathrm{p}}\otimes\mathrm{Grad}\mathfrak{e}_{\mathrm{p}}\right)\boldsymbol{F}_\gamma^{-1}\boldsymbol{F}_{\mathrm{p}}^{-1}\boldsymbol{\eta}^{-1}\right]. \tag{40}$$

We remark that $\boldsymbol{\Sigma}_\nu^{(\text{n-st})}$ is purely configurational, and it descends from the introduction of the micro-scale plasticity variable $\mathfrak{e}_{\mathrm{p}}$. Moreover, $\boldsymbol{\Sigma}_\nu^{(\text{n-st})}$ is independent of deformation, whereas it does depend on the growth and remodelling distortions, $\boldsymbol{F}_\gamma$ and $\boldsymbol{F}_{\mathrm{p}}$.

Remark 2. Tensor $\boldsymbol{\Sigma}_\nu$ and co-directionality. In our work, the deviatoric part of the generalised Mandel stress tensor, $\tilde{\boldsymbol{\Sigma}}_\nu$, is the stress tensor used to define $\boldsymbol{N}_\nu$ in (15). Therefore, it is the tensor with which the rate of plastic distortions, $\tilde{\boldsymbol{D}}_{\mathrm{p}}$, is co-directional. By virtue of the definition of $\boldsymbol{N}_\nu$, the direction of $\tilde{\boldsymbol{D}}_{\mathrm{p}}$ in the space of the symmetric second-order tensors is determined, partially, by the deviatoric part of the standard Mandel stress tensor, $\tilde{\boldsymbol{\Sigma}}_\nu^{(\mathrm{st})}$, and partially by $\tilde{\boldsymbol{\Sigma}}_\nu^{(\text{n-st})}$, which includes the contributions of the micro-scale "plasticity", through $\mathrm{Grad}\mathfrak{e}_{\mathrm{p}}$, and of the growth and remodelling distortions through $\boldsymbol{F}_\gamma$ and $\boldsymbol{F}_{\mathrm{p}}$, respectively. In the work of Anand et al.[44], instead, $\boldsymbol{N}_\nu$ is determined by $\boldsymbol{\Sigma}_\nu^{(\mathrm{st})}$ only.

By substituting (37) into (34), $\mathcal{D}_{\mathrm{R}}$ becomes

$$\begin{aligned}\mathcal{D}_{\mathrm{R}} = &\left\{-J_\gamma\left(\rho_{\mathrm{s}0}\Phi_{\mathrm{s}\nu}\frac{\partial\hat{\Psi}_{\mathrm{s}}^{(\mathrm{st})}}{\partial\boldsymbol{F}_{\mathrm{e}}}\boldsymbol{F}_{\mathrm{p}}^{-\mathrm{T}}\boldsymbol{F}_\gamma^{-\mathrm{T}}\right)+\boldsymbol{g}\boldsymbol{P}_{\mathrm{s}}\right\}:\dot{\boldsymbol{F}}+\left\{\Psi_{\mathrm{f}}-\Psi_{\mathrm{s}}+\frac{1}{3}\frac{\mathrm{tr}\left(\boldsymbol{\eta}\boldsymbol{\Sigma}_\nu\right)}{\rho_{\mathrm{s}0}\Phi_{\mathrm{s}\nu}}\right\}R_{\mathrm{s}}\\&+\left\{H_\varepsilon^{(\mathrm{i})}+J_\gamma\sqrt{\tfrac{3}{2}}\|\tilde{\boldsymbol{\Sigma}}_\nu\|_{\boldsymbol{\eta}}-J_\gamma A_\nu[\varepsilon_{\mathrm{p}}-\mathfrak{e}_{\mathrm{p}}]\right\}\dot{\varepsilon}_{\mathrm{p}}\\&+\left\{H_{\mathrm{p}}^{(\mathrm{i})}+J_\gamma A_\nu[\varepsilon_{\mathrm{p}}-\mathfrak{e}_{\mathrm{p}}]\right\}\dot{\mathfrak{e}}_{\mathrm{p}}+\left\{\Xi_{\mathrm{p}}-J_\gamma B_\nu\left[\left(\boldsymbol{F}_\gamma^{-1}\boldsymbol{B}_{\mathrm{p}}\boldsymbol{F}_\gamma^{-\mathrm{T}}\right)\mathrm{Grad}\mathfrak{e}_{\mathrm{p}}\right]\right\}\dot{\overline{\mathrm{Grad}\mathfrak{e}_{\mathrm{p}}}}\\&+\Phi_{\mathrm{f}}^{-1}\boldsymbol{Q}\boldsymbol{M}_{\mathrm{f}}+\boldsymbol{P}_{\mathrm{f}}:\boldsymbol{g}\mathrm{Grad}\boldsymbol{V}_{\mathrm{f}}+J\mathcal{D}_\gamma\geq 0\,.\end{aligned} \tag{41}$$

We study the dissipation inequality (41) by regarding the mass balance law (5) as a constraint[72,73], and appending it to $\mathcal{D}_{\mathrm{R}}$. To this end, we perform the Piola transformation of (5), thereby obtaining (see e.g.[36,72])

$$\mathcal{C}_{\mathrm{R}}\equiv\Phi_{\mathrm{s}}\boldsymbol{F}^{-\mathrm{T}}:\dot{\boldsymbol{F}}+\Phi_{\mathrm{f}}\boldsymbol{F}^{-\mathrm{T}}:\mathrm{Grad}\boldsymbol{V}_{\mathrm{f}}+J\Phi_{\mathrm{f}}^{-1}\boldsymbol{Q}\,\mathrm{Grad}(J^{-1}\Phi_{\mathrm{f}})-\left(\frac{1}{\rho_{\mathrm{s}0}}-\frac{1}{\rho_{\mathrm{f}0}}\right)R_{\mathrm{s}}=0, \tag{42}$$

where $\mathcal{C}_{\mathrm{R}}$ stands for "constraint". Then, we multiply (42) by a Lagrange multiplier, p, which plays the role of hydrostatic pressure, and we attach the resulting expression to (41). This leads to a "new" dissipation function, $\mathcal{D}_{\mathrm{R}}^{\mathrm{new}}\equiv\mathcal{D}_{\mathrm{R}}+p\mathcal{C}_{\mathrm{R}}$, that is equal to $\mathcal{D}_{\mathrm{R}}$, but is put in the form

$$\begin{aligned}\mathcal{D}_{\mathrm{R}}^{\mathrm{new}} = &\left\{-J_\gamma\left(\rho_{\mathrm{s}0}\Phi_{\mathrm{s}\nu}\frac{\partial\hat{\Psi}_{\mathrm{s}}^{(\mathrm{st})}}{\partial\boldsymbol{F}_{\mathrm{e}}}\boldsymbol{F}_{\mathrm{p}}^{-\mathrm{T}}\boldsymbol{F}_\gamma^{-\mathrm{T}}\right)+p\,\Phi_{\mathrm{s}}\boldsymbol{F}^{-\mathrm{T}}+\boldsymbol{g}\boldsymbol{P}_{\mathrm{s}}\right\}:\dot{\boldsymbol{F}}+\left\{p\,\Phi_{\mathrm{f}}\boldsymbol{F}^{-\mathrm{T}}+\boldsymbol{g}\boldsymbol{P}_{\mathrm{f}}\right\}:\mathrm{Grad}\boldsymbol{V}_{\mathrm{f}}\\&+\Phi_{\mathrm{f}}^{-1}\boldsymbol{Q}\left\{\boldsymbol{M}_{\mathrm{f}}+Jp\,\mathrm{Grad}(J^{-1}\Phi_{\mathrm{f}})\right\}+\left\{\left(\Psi_{\mathrm{f}}+\frac{p}{\rho_{\mathrm{f}0}}\right)-\left(\Psi_{\mathrm{s}}+\frac{p}{\rho_{\mathrm{s}0}}\right)+\frac{1}{3}\frac{\mathrm{tr}\left(\boldsymbol{\eta}\boldsymbol{\Sigma}_\nu\right)}{\rho_{\mathrm{s}0}\Phi_{\mathrm{s}\nu}}\right\}R_{\mathrm{s}}+J\mathcal{D}_\gamma\\&+\left\{H_\varepsilon^{(\mathrm{i})}+J_\gamma\sqrt{\tfrac{3}{2}}\,\|\tilde{\boldsymbol{\Sigma}}_\nu\|_{\boldsymbol{\eta}}-J_\gamma A_\nu[\varepsilon_{\mathrm{p}}-\mathfrak{e}_{\mathrm{p}}]\right\}\dot{\varepsilon}_{\mathrm{p}}\\&+\left\{H_{\mathrm{p}}^{(\mathrm{i})}+J_\gamma A_\nu[\varepsilon_{\mathrm{p}}-\mathfrak{e}_{\mathrm{p}}]\right\}\dot{\mathfrak{e}}_{\mathrm{p}}+\left\{\Xi_{\mathrm{p}}-J_\gamma B_\nu\left[\left(\boldsymbol{F}_\gamma^{-1}\boldsymbol{B}_{\mathrm{p}}\boldsymbol{F}_\gamma^{-\mathrm{T}}\right)\mathrm{Grad}\mathfrak{e}_{\mathrm{p}}\right]\right\}\dot{\overline{\mathrm{Grad}\mathfrak{e}_{\mathrm{p}}}}\geq 0.\end{aligned} \tag{43}$$

4.1 | Constitutive Laws

We require that the inequality (43) be valid for arbitrary values of $\dot{\boldsymbol{F}}$, $\mathrm{Grad}\boldsymbol{V}_\mathrm{f}$, $\dot{\mathrm{e}}_\mathrm{p}$, and $\overline{\dot{\mathrm{Grade}}_\mathrm{p}}$. Hence, the Coleman-Noll method implies the following identifications

$$\boldsymbol{P}_\mathrm{s} = -\Phi_\mathrm{s} p\, \boldsymbol{g}^{-1}\boldsymbol{F}^{-\mathrm{T}} + J_\gamma \left(\rho_{\mathrm{s}0}\Phi_{\mathrm{s}\nu}\boldsymbol{g}^{-1}\frac{\partial \hat{\Psi}_\mathrm{s}^{(\mathrm{st})}}{\partial \boldsymbol{F}_\mathrm{e}}\boldsymbol{F}_\mathrm{p}^{-\mathrm{T}}\boldsymbol{F}_\gamma^{-\mathrm{T}} \right), \tag{44a}$$

$$\boldsymbol{P}_\mathrm{f} = -\Phi_\mathrm{f} p\, \boldsymbol{g}^{-1}\boldsymbol{F}^{-\mathrm{T}}, \tag{44b}$$

$$H_\mathrm{p}^{(\mathrm{i})} = -J_\gamma A_\nu[\varepsilon_\mathrm{p} - \mathrm{e}_\mathrm{p}], \tag{44c}$$

$$\boldsymbol{\Xi}_\mathrm{p} = J_\gamma B_\nu \left[\boldsymbol{F}_\gamma^{-1}\boldsymbol{B}_\mathrm{p}\boldsymbol{F}_\gamma^{-\mathrm{T}}\right]\mathrm{Grade}_\mathrm{p}. \tag{44d}$$

In (44a), and in the sequel, the standard part of the solid phase Helmholtz free energy density, $\hat{\Psi}_\mathrm{s}^{(\mathrm{st})}$, is assumed to be of the Holmes-Mow type[59], i.e.,

$$\hat{\Psi}_\mathrm{s}^{(\mathrm{st})}(\boldsymbol{F}_\mathrm{e}) = \frac{\alpha_0}{\rho_{\mathrm{s}0}\Phi_{\mathrm{s}\nu}}\left\{\exp\left(\hat{f}(\boldsymbol{C}_\mathrm{e})\right) - 1\right\}, \tag{45}$$

where $\boldsymbol{C}_\mathrm{e} = \boldsymbol{F}_\mathrm{e}^{\mathrm{T}}.\boldsymbol{F}_\mathrm{e}$ is the elastic Cauchy-Green deformation tensor, α_0 is a material coefficient having physical units of energy per unit volume, and the function $\hat{f}$ is given by

$$\begin{aligned}\hat{f}(\boldsymbol{C}_\mathrm{e}) &= \check{f}(\hat{I}_1(\boldsymbol{C}_\mathrm{e}), \hat{I}_2(\boldsymbol{C}_\mathrm{e}), \hat{I}_3(\boldsymbol{C}_\mathrm{e})) \\ &= \alpha_1[\hat{I}_1(\boldsymbol{C}_\mathrm{e}) - 3] + \alpha_2[\hat{I}_2(\boldsymbol{C}_\mathrm{e}) - 3] - \alpha_3 \ln\left(\hat{I}_3(\boldsymbol{C}_\mathrm{e})\right),\end{aligned} \tag{46}$$

with $\hat{I}_1(\boldsymbol{C}_\mathrm{e})$, $\hat{I}_2(\boldsymbol{C}_\mathrm{e})$, and $\hat{I}_3(\boldsymbol{C}_\mathrm{e})$ denoting the first three principal invariants of $\boldsymbol{C}_\mathrm{e}$. The material parameters α_1, α_2, and α_3 are all assumed to be constant in this work. Moreover, it holds that $\alpha_1 + 2\alpha_2 = \alpha_3$ [59], and the following relations connect α_0, α_1, α_2, and α_3 with Lamé's elastic parameters of the material (see e.g. [56]):

$$\alpha_0 = \frac{2\mu + \lambda}{4\alpha_3}, \quad \alpha_1 = \alpha_3\frac{2\mu - \lambda}{2\mu + \lambda}, \quad \alpha_2 = \alpha_3\frac{\lambda}{2\mu + \lambda}. \tag{47}$$

In the forthcoming calculations, we set $\alpha_3 = 1$, and we give μ and λ the values reported in Table 1 .

We recognise the dissipative parts of $\boldsymbol{M}_\mathrm{f}$ and $H_\varepsilon^{(\mathrm{i})}$, which we identify with the following quantities

$$\boldsymbol{M}_\mathrm{f}^{(\mathrm{d})} = \boldsymbol{M}_\mathrm{f} + J p\,\mathrm{Grad}(J^{-1}\Phi_\mathrm{f}), \tag{48a}$$

$$H_\varepsilon^{(\mathrm{i,d})} = H_\varepsilon^{(\mathrm{i})} + J_\gamma\sqrt{\tfrac{3}{2}}\,\|\tilde{\boldsymbol{\Sigma}}_\nu\|_{\boldsymbol{\eta}} - J_\gamma A_\nu[\varepsilon_\mathrm{p} - \mathrm{e}_\mathrm{p}], \tag{48b}$$

and the dissipation inequality becomes

$$\mathcal{D}_\mathrm{R} = \Phi_\mathrm{f}^{-1}\boldsymbol{Q}\boldsymbol{M}_\mathrm{f}^{(\mathrm{d})} + H_\varepsilon^{(\mathrm{i,d})}\dot{\varepsilon}_\mathrm{p} + \left\{\left(\Psi_\mathrm{f} + \frac{p}{\rho_{\mathrm{f}0}}\right) - \left(\Psi_\mathrm{s} + \frac{p}{\rho_{\mathrm{s}0}}\right) + \frac{1}{3}\frac{\mathrm{tr}\left(\boldsymbol{\eta}\boldsymbol{\Sigma}_\nu\right)}{\rho_{\mathrm{s}0}\Phi_{\mathrm{s}\nu}}\right\} R_\mathrm{s} + J\mathcal{D}_\gamma \geq 0. \tag{49}$$

We notice that, in (48b), growth influences the expression of $H_\varepsilon^{(\mathrm{i,d})}$ through the determinant J_γ in the term $J_\gamma A_\nu[\varepsilon_\mathrm{p} - \mathrm{e}_\mathrm{p}]$.

According to (49), our model predicts that the system under study features three independent dissipative processes. The first one is due to the power loss associated with the resistance to the fluid flow and, under the hypothesis of negligible inertial forces, it leads to Darcy's law, i.e.,

$$\boldsymbol{M}_\mathrm{f}^{(\mathrm{d})} = \Phi_\mathrm{f}\boldsymbol{K}^{-1}\boldsymbol{Q}. \tag{50}$$

Equation (50) represents the material form of Darcy's law and, accordingly, the tensor $\boldsymbol{K}$ is the *material* permeability tensor of the medium, defined by

$$\boldsymbol{K}(X,t) = J(X,t)\boldsymbol{F}(X,t)\boldsymbol{k}(\chi(X,t),t)\boldsymbol{F}^{-\mathrm{T}}(X,t), \tag{51}$$

with $\boldsymbol{k}$ being the spatial permeability tensor. Finally, we remark that, in deriving (50), we have tacitly assumed that $\boldsymbol{K}$ is invertible, whereas sometimes this may not be necessarily the case. By substituting (50) into the first term on the right-hand-side of (49), we obtain that the dissipation due to fluid flow is always non-negative, i.e., for all $\boldsymbol{Q}$, it holds that $\Phi_\mathrm{f}^{-1}\boldsymbol{Q}\boldsymbol{M}_\mathrm{f}^{(\mathrm{d})} = \boldsymbol{K}^{-1} : (\boldsymbol{Q}\otimes\boldsymbol{Q}) \geq 0$, as long as $\boldsymbol{K}$ is positive-definite. Note that, by putting together the results (48a) and (50), $\boldsymbol{M}_\mathrm{f}$ is determined constitutively as

$$\boldsymbol{M}_\mathrm{f} = \Phi_\mathrm{f}\boldsymbol{K}^{-1}\boldsymbol{Q} - J p\,\mathrm{Grad}(J^{-1}\Phi_\mathrm{f}). \tag{52}$$

The second process contributing to the dissipation, $\mathcal{D}_{\mathrm{R}}$, is given by $H_{\varepsilon}^{(\mathrm{i,d})}\dot{\varepsilon}_{\mathrm{p}}$, which represents the power that the solid phase expends in order to remodel its internal structure by accumulating plastic strain ε_{p}. We assume that $H_{\varepsilon}^{(\mathrm{i,d})}\dot{\varepsilon}_{\mathrm{p}}$ is non-negative for all $\dot{\varepsilon}_{\mathrm{p}}$ and, since $\dot{\varepsilon}_{\mathrm{p}}$ is always non-negative by virtue of its own definition (see (18)), we conclude that $H_{\varepsilon}^{(\mathrm{i,d})}$ has to be non-negative too. In our work, we hypothesise that the tissue remodels in a rate-dependent way and, in particular, we assign $H_{\varepsilon}^{(\mathrm{i,d})}$ as

$$H_{\varepsilon}^{(\mathrm{i,d})} = J\tau_{\mathrm{p}}\dot{\varepsilon}_{\mathrm{p}}, \tag{53}$$

where τ_{p} is here taken as a strictly positive coefficient with the physical units of a generalised viscosity. By plugging (53) into (48b), we determine $H_{\varepsilon}^{(\mathrm{i})}$ through the constitutive law

$$H_{\varepsilon}^{(\mathrm{i})} = J\tau_{\mathrm{p}}\dot{\varepsilon}_{\mathrm{p}} - J_{\gamma}\sqrt{\tfrac{3}{2}}\,\|\tilde{\boldsymbol{\Sigma}}_{\nu}\|_{\boldsymbol{\eta}} + J_{\gamma}A_{\nu}[\varepsilon_{\mathrm{p}} - \mathfrak{e}_{\mathrm{p}}]. \tag{54}$$

The third dissipative phenomenon is given by growth, and is represented by the last two summands on the right-hand-side of (49), which we denote by $\mathcal{D}_{\mathrm{g}}$ and refer to as the "growth part of $\mathcal{D}_{\mathrm{R}}$". In contrast to what we have done for the other dissipative processes, and even though the terms between braces in (49) may be understood as the generalised force power-conjugate to $\dot{\gamma}/\gamma$ through R_{s}, we do not try to look for information on R_{s} from the requirement that $\mathcal{D}_{\mathrm{g}}$ has to be non-negative. Rather, following[4,6,24,33,37,53,54], we enforce a phenomenological law for R_{s}, which is translated into the kinematic constraint (23) on $\dot{\gamma}/\gamma$, and we use $\mathcal{D}_{\gamma}$ to adjust $\mathcal{D}_{\mathrm{g}}$ and guarantee that it remains non-negative. We emphasise that, although this path may seem artificial, it can be justified by noticing that $\mathcal{D}_{\gamma}$ represents processes, related to growth, that are not resolved explicitly by our model but that are necessary for growth to occur. In fact, a motivation for introducing a term like $\mathcal{D}_{\gamma}$ in the dissipation inequality of a growth problem can be found in[66].

4.2 | Dynamic Equations

By adopting the material form of the momentum balance laws (28a) and (28b), and by invoking the force balance $\boldsymbol{m}_{\mathrm{s}} + \boldsymbol{m}_{\mathrm{f}} = \boldsymbol{0}$, we obtain

$$-\boldsymbol{g}^{-1}\boldsymbol{F}^{-\mathrm{T}}\boldsymbol{M}_{\mathrm{f}} - \mathrm{Div}\boldsymbol{P}_{\mathrm{s}} = \boldsymbol{0}, \tag{55a}$$

$$\boldsymbol{g}^{-1}\boldsymbol{F}^{-\mathrm{T}}\boldsymbol{M}_{\mathrm{f}} - \mathrm{Div}\boldsymbol{P}_{\mathrm{f}} = \boldsymbol{0}, \tag{55b}$$

where the constitutive expressions of $\boldsymbol{P}_{\mathrm{s}}$, $\boldsymbol{P}_{\mathrm{f}}$, and $\boldsymbol{M}_{\mathrm{f}}$ are given in (44a), (44b), and (52), respectively. Furthermore, by adding together (55a) with (55b), and using the explicit expression for $\boldsymbol{M}_{\mathrm{f}}$ in (55b), we find

$$\mathrm{Div}(\boldsymbol{P}_{\mathrm{s}} + \boldsymbol{P}_{\mathrm{f}}) = \boldsymbol{0}, \tag{56a}$$

$$\boldsymbol{K}^{-1}\boldsymbol{Q} + \mathrm{Grad}\,p = \boldsymbol{0}. \tag{56b}$$

We exploit now the generalised force balance (28c), which becomes $H_{\varepsilon}^{(\mathrm{i})} = H_{\varepsilon}^{(\mathrm{e})}$ in material form and, by replacing $H_{\varepsilon}^{(\mathrm{i})}$ with the right-hand-side of (54), we determine an evolution law for ε_{p}, i.e.,

$$J\tau_{\mathrm{p}}\dot{\varepsilon}_{\mathrm{p}} - J_{\gamma}\sqrt{\tfrac{3}{2}}\,\|\tilde{\boldsymbol{\Sigma}}_{\nu}\|_{\boldsymbol{\eta}} + J_{\gamma}A_{\nu}[\varepsilon_{\mathrm{p}} - \mathfrak{e}_{\mathrm{p}}] = H_{\varepsilon}^{(\mathrm{e})}. \tag{57}$$

To close this equation, we prescribe $H_{\varepsilon}^{(\mathrm{e})}$ as

$$H_{\varepsilon}^{(\mathrm{e})} = -\left[J\sigma_{\mathrm{th}} + J_{\gamma}Z_{\nu}[\varepsilon_{\mathrm{p}} - \mathfrak{e}_{\mathrm{p}}]\right], \tag{58}$$

where σ_{th} is a threshold stress, and Z_{ν} is a material parameter[44]. Hence, setting $\lambda_{\mathrm{p}} = 1/\tau_{\mathrm{p}}$, Equation (57) takes on the form

$$\dot{\varepsilon}_{\mathrm{p}} = \frac{\lambda_{\mathrm{p}}}{J}\left\{\left(J_{\gamma}\sqrt{\tfrac{3}{2}}\,\|\tilde{\boldsymbol{\Sigma}}_{\nu}\|_{\boldsymbol{\eta}} - J\sigma_{\mathrm{th}}\right) - J_{\gamma}(A_{\nu} + Z_{\nu})[\varepsilon_{\mathrm{p}} - \mathfrak{e}_{\mathrm{p}}]\right\}. \tag{59}$$

The last dynamic equation is supplied by (28d). Recalling that, in the present framework, the external force $h_{\mathrm{p}}^{(\mathrm{e})}$ is zero, the material form of (28d) reads

$$H_{\mathrm{p}}^{(\mathrm{i})} - \mathrm{Div}\,\boldsymbol{\Xi}_{\mathrm{p}} = 0. \tag{60}$$

Hence, by substituting (44c) and (44d) into (60), we obtain

$$-J_{\gamma}A_{\nu}[\varepsilon_{\mathrm{p}} - \mathfrak{e}_{\mathrm{p}}] - \mathrm{Div}\left(J_{\gamma}B_{\nu}\left[\boldsymbol{F}_{\gamma}^{-1}\boldsymbol{B}_{\mathrm{p}}\boldsymbol{F}_{\gamma}^{-\mathrm{T}}\right]\mathrm{Grad}\mathfrak{e}_{\mathrm{p}}\right) = 0. \tag{61}$$

In particular, since we take $\boldsymbol{F}_\gamma$ as $\boldsymbol{F}_\gamma = \gamma \boldsymbol{I}$, (61) acquires the equivalent form

$$-\gamma^3 A_\nu[\varepsilon_\mathrm{p} - \mathrm{e}_\mathrm{p}] - \mathrm{Div}\left(\gamma B_\nu \boldsymbol{B}_\mathrm{p} \mathrm{Grad}\mathrm{e}_\mathrm{p}\right) = 0. \tag{62}$$

Remark 3. The equation for e_p. The result (62) is our generalisation to Equation (4.40) of Anand et al.[44], which, in our notation, and assuming constant values for A_ν and B_ν, would read

$$-A_\nu[\varepsilon_\mathrm{p} - \mathrm{e}_\mathrm{p}] - B_\nu \Delta \mathrm{e}_\mathrm{p} = 0 \quad \Rightarrow \quad \mathrm{e}_\mathrm{p} - l_\nu^2 \Delta \mathrm{e}_\mathrm{p} = \varepsilon_\mathrm{p}, \quad l_\nu = \sqrt{B_\nu / A_\nu}, \tag{A}$$

with Δ being the Laplace operator, and l_ν the characteristic length scale associated with the micro-scale plasticity variable, e_p. For a given distribution of ε_p, Equation (A) returns a "regularised" version of ε_p. In particular, since e_p is required to satisfy Neumann-zero boundary conditions, if ε_p is constant in $\mathscr{B}$, then the unique solution to (A) is the constant solution $\mathrm{e}_\mathrm{p} = \varepsilon_\mathrm{p}$. However, when ε_p is strongly localised, the output of (A), i.e., e_p, tends to be a lot more homogeneous, the more l_ν increases.

Our generalisation to (A) is twofold: first, the plastic-like distortions determine the evolution of e_p both through ε_p and through the second-order tensor $\boldsymbol{B}_\mathrm{p} = \boldsymbol{F}_\mathrm{p}^{-1}.\boldsymbol{F}_\mathrm{p}^{-\mathrm{T}}$. While ε_p is an input for (A), $\boldsymbol{B}_\mathrm{p}$ modulates, together with the growth parameter γ, the non-locality of e_p, which is thus measured by the tensorial coefficient $\gamma B_\nu \boldsymbol{B}_\mathrm{p}$. We notice that the occurrence of this coefficient is due to the last term in the definition of $\hat{\Psi}_\mathrm{s}$ given in (36). Switching to the Eulerian formalism, and using the identity $\mathrm{Grad}\mathrm{e}_\mathrm{p}(X,t) = (\nabla \mathrm{e}_\mathrm{p}(\chi(X,t),t)\boldsymbol{F}(X,t)$, this term reads

$$\tfrac{1}{2} b_0 \boldsymbol{b}_\mathrm{e} \,:\, \nabla \mathrm{e}_\mathrm{p} \otimes \nabla \mathrm{e}_\mathrm{p},$$

thereby meaning that, in the spatial description, the non-locality of the micro-"plastic" variable, e_p, is modulated by the elastic left Cauchy-Green deformation tensor, $\boldsymbol{b}_\mathrm{e} = \boldsymbol{F}_\mathrm{e}.\boldsymbol{F}_\mathrm{e}^\mathrm{T}$. To eliminate $\boldsymbol{B}_\mathrm{p}$ from (62), and obtain a model closer to that of Anand et al.[44], we should substitute $\boldsymbol{b}_\mathrm{e}$ with the left Cauchy-Green deformation tensor $\boldsymbol{b} = \boldsymbol{F}.\boldsymbol{F}^\mathrm{T}$. Such a choice would lead to replace the last term of (36) with

$$\tfrac{1}{2} b_0 \boldsymbol{G}^{-1} \,:\, \mathrm{Grad}\mathrm{e}_\mathrm{p} \otimes \mathrm{Grad}\mathrm{e}_\mathrm{p},$$

and would have the consequence of defining the unit tensor $\boldsymbol{N}_\nu$ just in terms of the standard Mandel stress tensor, $\boldsymbol{\Sigma}_\nu^{(\mathrm{st})}$ (see Remark 2). We recall that $\boldsymbol{G}$ denotes here the natural material metric tensor associated with $\mathscr{B}$.

The second aspect of our generalisation is related to the fact that, in our model, the evolution of e_p is influenced by the growth parameter, γ, which couples with the coefficients A_ν and B_ν, thereby rescaling the characteristic length scale associated with e_p in a generally inhomogeneous way, i.e., as $l_\nu \to l = l_\nu \|\boldsymbol{B}_\mathrm{p}\|_{\boldsymbol{G}}^{1/2}/\gamma$, so that, for a given l_ν, the condition $\gamma > 1$ tends to reduce the length scale associated with e_p. Note that $\|\boldsymbol{B}_\mathrm{p}\|_{\boldsymbol{G}} = [\mathrm{tr}(\boldsymbol{G}\boldsymbol{B}_\mathrm{p}\boldsymbol{G}\boldsymbol{B}_\mathrm{p})]^{1/2}$.

Remark 4. Choice of $H_\varepsilon^{(\mathrm{e})}$. In the literature on remodelling (see e.g.[11,13,19]), when an external force, like $H_\varepsilon^{(\mathrm{e})}$, is taken into account, it is often chosen in such a way that a homeostatic state exists for the system under study. If we had followed such philosophy, we should have admitted homeostatic terms for ε_p and e_p, denoted by $\varepsilon_\mathrm{p}^{(\mathrm{h})}$ and $\mathrm{e}_\mathrm{p}^{(\mathrm{h})}$, and we should have expressed $H_\varepsilon^{(\mathrm{e})}$ as

$$H_\varepsilon^{(\mathrm{e})} = -J_\gamma \sqrt{\tfrac{3}{2}}\, \|\tilde{\boldsymbol{\Sigma}}_\nu^{(\mathrm{h})}\|_{\boldsymbol{\eta}} + J_\gamma A_\nu[\varepsilon_\mathrm{p}^{(\mathrm{h})} - \mathrm{e}_\mathrm{p}^{(\mathrm{h})}], \tag{63}$$

where $\tilde{\boldsymbol{\Sigma}}_\nu^{(\mathrm{h})}$ is the Mandel-like stress tensor in homeostatic conditions (that is, when its arguments attain the homeostatic state). This consideration notwithstanding, in our work we opted for the expression (58) because, in order to formulate a proof of concept for our problem, we needed to remain as close as possible to the framework supplied by[44].

Remark 5. Evolution law for ε_p. Equation (58) represents an essential difference with respect to the evolution law for ε_p given by[44]. Indeed, Anand et al.[44] set $H_\varepsilon^{(\mathrm{i})} = H_\varepsilon^{(\mathrm{e})} = 0$, and assign $H_\varepsilon^{(\mathrm{i,d})}$ constitutively as a law that plays the role of an *effective yield stress*, i.e., $H_\varepsilon^{(\mathrm{i,d})} = J\sigma_\mathrm{th} + J_\gamma Z_\nu[\varepsilon_\mathrm{p} - \mathrm{e}_\mathrm{p}]$, where $\sigma_\mathrm{th} > 0$ plays the role of the *"conventional yield stress"*[44][3], while $Z_\nu > 0$ is a model parameter defining the purely dissipative part of $H_\varepsilon^{(\mathrm{i,d})}$. By doing this, the Authors rewrite the balance equation $H_\varepsilon^{(\mathrm{i})} = H_\varepsilon^{(\mathrm{e})}$ in terms of a yield function of the type $\mathfrak{f} = J_\gamma \sqrt{\frac{3}{2}} \|\tilde{\boldsymbol{\Sigma}}_\nu\|_{\boldsymbol{\eta}} - \left(J\sigma_\mathrm{th} + J_\gamma(A_\nu + Z_\nu)[\varepsilon_\mathrm{p} - \mathrm{e}_\mathrm{p}]\right)$. In particular, according to the theory of Anand et al.[44], it occurs that $\dot{\varepsilon}_\mathrm{p} = 0$, if $\mathfrak{f} < 0$, and $\dot{\varepsilon}_\mathrm{p} > 0$, if $\mathfrak{f} = 0$. This approach is equivalent to the

[3] Note that, differently from what is assumed here, Anand et al.[44] hypothesise that the conventional yield stress is a monotonically decreasing function of ε_p, because they are interested in studying the phenomenon of *strain-softening*.

elasto-plastic problem in the Karush-Kuhn-Tucker form, i.e.,

$$\mathfrak{f} \leq 0, \qquad \dot{\varepsilon}_{\mathrm{p}} \geq 0, \qquad \mathfrak{f}\,\dot{\varepsilon}_{\mathrm{p}} = 0, \tag{64}$$

where $\dot{\varepsilon}_{\mathrm{p}}$ is determined by means of the consistency condition $\dot{\varepsilon}_{\mathrm{p}}\dot{\mathfrak{f}} = 0$, when $\mathfrak{f} = 0$. If, in our work, we had followed the approach outlined by Anand et al.[44], we would have found a very complicated evolution law for ε_{p}, especially from the computational point of view. To circumvent this technical difficulty, we have proposed a modification to the model, i.e., we have assumed $H_{\varepsilon}^{(\mathrm{i})} = H_{\varepsilon}^{(\mathrm{e})} \neq 0$ and, in order to obtain an evolution law for ε_{p} of the type $J\tau_{\mathrm{p}}\dot{\varepsilon}_{\mathrm{p}} = \mathfrak{f}$ (cf. Equation (57)), with $\mathfrak{f}$ defined as done by Anand et al.[44], we have exploited the "freedom" we have to express $H_{\varepsilon}^{(\mathrm{e})}$ as in (58). A last comment pertains to the terms λ_{p}/J and $J\sigma_{\mathrm{th}}$ featuring in Equation (59): if λ_{p} and σ_{th} are such that $\lambda_{\mathrm{p}}/J_{\mathrm{e}} \equiv \Lambda_{\mathrm{p}}$ and $J_{\mathrm{e}}\sigma_{\mathrm{th}} \equiv \Sigma_{\mathrm{th}}$ are constants, then it holds that $\lambda_{\mathrm{p}}/J = \Lambda_{\mathrm{p}}/J_{\gamma}$ and $J\sigma_{\mathrm{th}} = J_{\gamma}\Sigma_{\mathrm{th}}$. In this case, J_{γ} does not feature explicitly in Equation (59), which becomes $\dot{\varepsilon}_{\mathrm{p}} = \Lambda_{\mathrm{p}}\tilde{\mathfrak{f}}$, where we have set $\tilde{\mathfrak{f}} \equiv \mathfrak{f}/J_{\gamma}$. In this case, Σ_{th} acquires the meaning of the yield stress that is used in the yield criteria formulated in terms of the norm of the Mandel stress tensor (see e.g.[43]). We remark, however, that solving $\dot{\varepsilon}_{\mathrm{p}} = \Lambda_{\mathrm{p}}\tilde{\mathfrak{f}}$ in lieu of (59) leads, in our work, to no appreciable differences in the simulation results.

5 | MODEL EQUATIONS AND BENCHMARK TEST

In this section, we summarise all the model equations and their corresponding unknowns, we highlight the fundamental hypotheses adopted to simplify our simulations, and we describe the benchmark problem used for testing our model.

5.1 | Summary of the model equations

The first equation of the problem is given by (56a), i.e., the momentum balance law for the mixture as a whole, and its associated unknown is given by the solid phase motion, χ. The second equation determines the pressure, p, and is supplied by the mass balance law (8d), in which, coherently with (56b), $\boldsymbol{Q}$ is expressed as $\boldsymbol{Q} = -\boldsymbol{K}\mathrm{Grad}p$. The right-hand-side of (8d) is set equal to zero on the basis of the assumption that, in tumours, the mass densities $\rho_{\mathrm{s}0}$ and $\rho_{\mathrm{f}0}$ are approximately the same. The third equation is the mass balance of the proliferating cells (8a), and its corresponding unknown is the mass fraction ω_{p}. The fourth equation is in the mass fraction of the nutrients, ω_{N}, and is obtained from (8c) by using the identities $\Phi_{\mathrm{f}} = J - J_{\gamma}\Phi_{\mathrm{s}\nu}$ and $\boldsymbol{Y}_{\mathrm{N}} = -\rho_{\mathrm{f}0}\boldsymbol{D}\mathrm{Grad}\,\omega_{\mathrm{N}}$. The fifth equation descends for the mass balance law of the solid phase and, by assigning the mass source R_{s} phenomenologically, it puts a constraint on the growth parameter, γ, which is thus bound to comply with (23). Except for the sources and sinks of mass, which are defined in a slightly different way in our work, the five equations mentioned so far are the same as those studied by Mascheroni et al.[24] and Di Stefano et al.[54].

The evolution of the plastic distortions is described by the dynamic equation (59), which determines ε_{p}, and by the constraint on $\boldsymbol{F}_{\mathrm{p}}$ placed by (20). These add two more equations to the previous five. Finally, the equation for the micro-scale "plasticity" variable, e_{p}, is supplied by (62).

In conclusion, by putting together all the laws enumerated up to now, we obtain

$$\mathrm{Div}(\boldsymbol{P}_{\mathrm{f}} + \boldsymbol{P}_{\mathrm{s}}) = \boldsymbol{0}, \tag{65a}$$

$$\mathrm{Div}\,(\boldsymbol{K}\mathrm{Grad}p) = \dot{\boldsymbol{J}}, \tag{65b}$$

$$\rho_{\mathrm{s}0}J_{\gamma}\Phi_{\mathrm{s}\nu}\dot{\omega}_{\mathrm{p}} = R_{\mathrm{pn}} + R_{\mathrm{fp}} - R_{\mathrm{s}}\omega_{\mathrm{p}}, \tag{65c}$$

$$\rho_{\mathrm{f}0}[J - J_{\gamma}\Phi_{\mathrm{s}\nu}]\dot{\omega}_{\mathrm{N}} + \rho_{\mathrm{f}0}\boldsymbol{Q}\,\mathrm{Grad}\omega_{\mathrm{N}} = \mathrm{Div}\left(\rho_{\mathrm{f}0}\boldsymbol{D}\,\mathrm{Grad}\,\omega_{\mathrm{N}}\right) + R_{\mathrm{Np}} + R_{\mathrm{s}}\omega_{\mathrm{N}}, \tag{65d}$$

$$\dot{\gamma} = \frac{R_{\mathrm{s}}}{3\rho_{\mathrm{s}0}\Phi_{\mathrm{s}\nu}\gamma^2}, \tag{65e}$$

$$\dot{\varepsilon}_{\mathrm{p}} = \frac{\lambda_{\mathrm{p}}}{J}\left\{\left(J_{\gamma}\sqrt{\tfrac{3}{2}}\|\tilde{\boldsymbol{\Sigma}}_{\nu}\|_{\boldsymbol{\eta}} - J\sigma_{\mathrm{th}}\right) - J_{\gamma}(A_{\nu} + Z_{\nu})[\varepsilon_{\mathrm{p}} - \mathrm{e}_{\mathrm{p}}]\right\}, \tag{65f}$$

$$\dot{\boldsymbol{F}}_{\mathrm{p}} = \left(\sqrt{\tfrac{3}{2}}\,\dot{\varepsilon}_{\mathrm{p}}\boldsymbol{\eta}^{-1}\boldsymbol{N}_{\nu}\right)\boldsymbol{F}_{\mathrm{p}}, \tag{65g}$$

$$\mathrm{Div}\left(\gamma B_{\nu}\boldsymbol{B}_{\mathrm{p}}\mathrm{Grad}\mathrm{e}_{\mathrm{p}}\right) - \gamma^3 A_{\nu}\mathrm{e}_{\mathrm{p}} = -\gamma^3 A_{\nu}\varepsilon_{\mathrm{p}}, \tag{65h}$$

which constitutes a system of 18 scalar equations in the 18 unknowns

$$\mathcal{U} = \{\chi, p, \omega_{\mathrm{p}}, \omega_{\mathrm{N}}, \gamma, \varepsilon_{\mathrm{p}}, \boldsymbol{F}_{\mathrm{p}}, \mathrm{e}_{\mathrm{p}}\}. \tag{66}$$

For ensuring the non-negativity of $\dot{\varepsilon}_{\mathrm{p}}$ at all times and at all points, we solve (65f) numerically by taking the positive part of its right-hand-side. Moreover, to close the problem, we prescribe the permeability tensor and the diffusion tensor[54,59,74,75],

$$\boldsymbol{K} = J k_0 \boldsymbol{C}^{-1}, \quad k_0 = k_{0\mathrm{R}} \left[\frac{J - J_\gamma \Phi_{\mathrm{sv}}}{J_\gamma \varphi_{\mathrm{f}0}} \right]^{m_0} \exp\left(\frac{m_1}{2} \left[\frac{J^2 - J_\gamma^2}{J_\gamma^2} \right] \right), \tag{67a}$$

$$\boldsymbol{D} = J d_0 \boldsymbol{C}^{-1}, \quad d_0 = \frac{J - J_\gamma \Phi_{\mathrm{sv}}}{J} d_{0\mathrm{R}}, \tag{67b}$$

as well as the sources and sinks of mass[24,54], i.e.,

$$R_{\mathrm{pn}} = -J\zeta_{\mathrm{pn}} \left\langle 1 - \frac{\omega_{\mathrm{N}}}{\omega_{\mathrm{Ncr}}} \right\rangle_+ \frac{J_\gamma \Phi_{\mathrm{sv}}}{J} \omega_{\mathrm{p}}, \tag{68a}$$

$$R_{\mathrm{fp}} = J\zeta_{\mathrm{fp}} \left\langle \frac{\omega_{\mathrm{N}} - \omega_{\mathrm{Ncr}}}{\omega_{\mathrm{Nenv}} - \omega_{\mathrm{Ncr}}} \right\rangle_+ \left[1 - \frac{\delta_1 \langle \wp \rangle_+}{\delta_2 + \langle \wp \rangle_+} \right] \frac{J - J_\gamma \Phi_{\mathrm{sv}}}{J \varphi_{\mathrm{f}0}} \frac{J_\gamma \Phi_{\mathrm{sv}}}{J} \omega_{\mathrm{p}}, \tag{68b}$$

$$R_{\mathrm{s}} = R_{\mathrm{fp}} + R_{\mathrm{nf}}, \tag{68c}$$

$$R_{\mathrm{nf}} = -J\zeta_{\mathrm{nf}} [1 - \omega_{\mathrm{p}}] \frac{J_\gamma \Phi_{\mathrm{sv}}}{J}, \tag{68d}$$

$$R_{\mathrm{Np}} = -J\zeta_{\mathrm{Np}} \frac{\omega_{\mathrm{N}}}{\omega_{\mathrm{N}} + \omega_{\mathrm{N}0}} \frac{J_\gamma \Phi_{\mathrm{sv}}}{J} \omega_{\mathrm{p}}. \tag{68e}$$

Since the expressions of R_{pn}, R_{fp}, R_{nf}, and R_{Np} have been already commented in previous works[24,54], we do not spend any more words here on their derivation. We recall, however, that the operator $\langle \cdot \rangle_+$ returns the positive part of its argument, and that ω_{Ncr} denotes a critical value of the mass fraction of the nutrients, below which the proliferating cells tend to be necrotic (that is, $R_{\mathrm{pn}} < 0$), whereas ω_{Nenv} represents the mass fraction of the nutrients in the "environment". Both ω_{Nenv} and ω_{Ncr} are regarded as constant parameters in our work, and it is assumed that the condition $\omega_{\mathrm{Nenv}} > \omega_{\mathrm{Ncr}}$ is always respected, so that also R_{fp} is deactivated, i.e., $R_{\mathrm{fp}} = 0$, for $\omega_{\mathrm{N}} < \omega_{\mathrm{Ncr}}$. Moreover, looking at the definition of R_{fp}, and bearing in mind that, for $\omega_{\mathrm{N}} > \omega_{\mathrm{Ncr}}$, R_{fp} describes the positive variation of mass of the tissue's solid phase, we notice that the factor

$$\left[1 - \frac{\delta_1 \langle \wp \rangle_+}{\delta_2 + \langle \wp \rangle_+} \right]$$

accounts for mechanotransduction through the action of the stress $\langle \wp \rangle_+$. Comparing this result with the works of Mascheroni et al.[24] and Di Stefano et al.[54], we notice that our model suggests a slightly different interpretation of mechanotransduction. Indeed, while Mascheroni et al.[24] and Di Stefano et al.[54] prescribe $\wp$ as $\wp = -(1/3)\mathrm{tr}(\boldsymbol{g}\boldsymbol{\sigma}_{\mathrm{sc}})$, where $\boldsymbol{\sigma}_{\mathrm{sc}} = J^{-1} \boldsymbol{P}_{\mathrm{sc}} \boldsymbol{F}^{\mathrm{T}}$ is the constitutive part of the solid phase Cauchy stress, and, accordingly, $\boldsymbol{P}_{\mathrm{sc}}$ is defined by

$$\boldsymbol{P}_{\mathrm{sc}} = J_\gamma \left(\rho_{\mathrm{s}0} \Phi_{\mathrm{sv}} \boldsymbol{g}^{-1} \frac{\partial \hat{\Psi}_{\mathrm{s}}^{(\mathrm{st})}}{\partial \boldsymbol{F}_{\mathrm{e}}} (\boldsymbol{F} \boldsymbol{F}_\gamma^{-1} \boldsymbol{F}_{\mathrm{p}}^{-1}) \boldsymbol{F}_{\mathrm{p}}^{-\mathrm{T}} \boldsymbol{F}_\gamma^{-\mathrm{T}} \right) \equiv \mathcal{P}_{\mathrm{sc}}(\boldsymbol{F}, \boldsymbol{F}_\gamma, \boldsymbol{F}_{\mathrm{p}}), \tag{69}$$

in our approach $\wp$ is taken as $\wp = -(1/3)\mathrm{tr}(\boldsymbol{g}\boldsymbol{\sigma}_{\mathrm{eff}})$ (see also[19]), with

$$\begin{aligned} \boldsymbol{\sigma}_{\mathrm{eff}} &= \boldsymbol{\sigma}_{\mathrm{sc}} + \frac{1}{J_{\mathrm{e}}} \boldsymbol{g}^{-1} \boldsymbol{F}_{\mathrm{e}}^{-\mathrm{T}} \boldsymbol{\eta} \boldsymbol{\Sigma}_\nu^{(\mathrm{n\text{-}st})} \boldsymbol{F}_{\mathrm{e}}^{\mathrm{T}} = \frac{1}{J_{\mathrm{e}}} \boldsymbol{g}^{-1} \boldsymbol{F}_{\mathrm{e}}^{-\mathrm{T}} \boldsymbol{\eta} \boldsymbol{\Sigma}_\nu^{(\mathrm{st})} \boldsymbol{F}_{\mathrm{e}}^{\mathrm{T}} + \frac{1}{J_{\mathrm{e}}} \boldsymbol{g}^{-1} \boldsymbol{F}_{\mathrm{e}}^{-\mathrm{T}} \boldsymbol{\eta} \boldsymbol{\Sigma}_\nu^{(\mathrm{n\text{-}st})} \boldsymbol{F}_{\mathrm{e}}^{\mathrm{T}} \\ &= \frac{1}{J_{\mathrm{e}}} \boldsymbol{g}^{-1} \boldsymbol{F}_{\mathrm{e}}^{-\mathrm{T}} \boldsymbol{\eta} \boldsymbol{\Sigma}_\nu \boldsymbol{F}_{\mathrm{e}}^{\mathrm{T}}. \end{aligned} \tag{70}$$

In other words, while the works done by Mascheroni et al.[24] and Di Stefano et al.[54] the stress used to express the mechanotransduction is the classical $\boldsymbol{\sigma}_{\mathrm{sc}}$, we propose here to adopt the *effective Cauchy stress*, $\boldsymbol{\sigma}_{\mathrm{eff}}$, which captures both $\boldsymbol{\sigma}_{\mathrm{sc}}$ and the non-standard, purely configurational contribution $\boldsymbol{\Sigma}_\nu^{(\mathrm{n\text{-}st})}$. Our point is that, since in our approach $\boldsymbol{\Sigma}_\nu$ is (power-)conjugate to the growth rate $\dot{\gamma}/\gamma$ (through R_{s}) and to $\dot{\varepsilon}_{\mathrm{p}}$ (see (37)), it might be a more natural representative of the stress responsible for modulating growth. This consideration notwithstanding, for the parameters chosen in our simulations, the contribution of $\boldsymbol{\Sigma}_\nu^{(\mathrm{n\text{-}st})}$ is very marginal with respect to the standard measures of stress, and its contribution is thus not much appreciable.

5.2 | Benchmark problem

The benchmark problem is essentially the same as the one computed in Di Stefano et al.[54], with the major difference that we are now considering also plastic distortions and the role of micro-plasticity. Hence, by adapting a study originally designed

by Ambrosi and Mollica[53], we consider the case of volumetric growth in a cylindrical sample of isotropic material. For this purpose, we introduce the systems of cylindrical coordinates (R, Θ, Z) and (r, θ, z), which cover the reference and current configuration, respectively. For both systems, the first coordinate is radial, the second one is circumferential, and the third one is axial.

We assume that the radius of the specimen is preserved, and that only its length varies along the axial direction. Hence, we eliminate any rigid rotation about the principal axis. These restrictions imply that the momentum balance law (65a) reduces to a scalar equation in Z, and that the deformation gradient tensor becomes $\boldsymbol{F} = \boldsymbol{e}_r \otimes \boldsymbol{E}^R + \boldsymbol{e}_\theta \otimes \boldsymbol{E}^\Theta + (1 + \frac{\partial u}{\partial Z})\boldsymbol{e}_z \otimes \boldsymbol{E}^Z$, where u is the field of axial displacements. We note that $\{\boldsymbol{E}^R, \boldsymbol{E}^\Theta, \boldsymbol{E}^Z\}$ and $\{\boldsymbol{e}_r, \boldsymbol{e}_\theta, \boldsymbol{e}_z\}$ are the co-vector and vector bases associated with the system of cylindrical coordinates (R, Θ, Z) and (r, θ, z), respectively.

We impose the following boundary conditions on Equations (65a)–(65h)

$$(-\boldsymbol{J}p\boldsymbol{g}^{-1}\boldsymbol{F}^{-\mathrm{T}} + \boldsymbol{P}_{\mathrm{sc}}).\boldsymbol{N}_{\mathrm{A}} = \boldsymbol{0}, \qquad \text{on } (\partial\mathscr{B})_{\mathrm{Left}} \text{ and } (\partial\mathscr{B})_{\mathrm{Right}}, \tag{71a}$$

$$p = 0, \qquad \text{on } (\partial\mathscr{B})_{\mathrm{Left}} \text{ and } (\partial\mathscr{B})_{\mathrm{Right}}, \tag{71b}$$

$$(-\boldsymbol{K}\mathrm{Grad}\, p).\boldsymbol{N}_{\mathrm{C}} = 0, \qquad \text{on } (\partial\mathscr{B})_{\mathrm{C}}, \tag{71c}$$

$$(-\rho_{\mathrm{f}}\boldsymbol{D}\mathrm{Grad}\, \omega_{\mathrm{N}}).\boldsymbol{N}_{\mathrm{C}} = 0, \qquad \text{on } (\partial\mathscr{B})_{\mathrm{C}}, \tag{71d}$$

$$\omega_{\mathrm{N}} = \omega_{\mathrm{Nenv}}, \qquad \text{on } (\partial\mathscr{B})_{\mathrm{Left}} \text{ and } (\partial\mathscr{B})_{\mathrm{Right}}, \tag{71e}$$

$$(\gamma B_\nu \boldsymbol{B}_{\mathrm{p}}\mathrm{Grad}\mathbf{e}_{\mathrm{p}}).\boldsymbol{N} = 0, \qquad \text{on } \partial\mathscr{B}, \tag{71f}$$

where $\partial\mathscr{B} = (\partial\mathscr{B})_{\mathrm{Left}} \cup (\partial\mathscr{B})_{\mathrm{C}} \cup (\partial\mathscr{B})_{\mathrm{Right}}$, $(\partial\mathscr{B})_{\mathrm{C}}$ is the lateral boundary of the cylinder, $(\partial\mathscr{B})_{\mathrm{Left}}$ and $(\partial\mathscr{B})_{\mathrm{Right}}$ are the left and right surface cross-sections at $Z = -L/2$ and $Z = L/2$, respectively, and L is the initial length of the cylinder. Moreover, $\boldsymbol{N}_{\mathrm{A}}$, $\boldsymbol{N}_{\mathrm{C}}$, and $\boldsymbol{N}$ are fields of unit vectors normal to $(\partial\mathscr{B})_{\mathrm{Left}}$ and $(\partial\mathscr{B})_{\mathrm{Right}}$, $(\partial\mathscr{B})_{\mathrm{C}}$, and $\partial\mathscr{B}$, respectively.

Equations (71a) and (71b) mean that the left and right ends of the cylinder are free boundaries. The relations (71c) and (71d) are enforced to express that $(\partial\mathscr{B})_{\mathrm{C}}$ is undeformable and impermeable to the fluid and to the nutrients, respectively. Equation (71e) is a Dirichlet condition specifying that there always exists a constant availability of nutrients on the boundaries $(\partial\mathscr{B})_{\mathrm{Left}}$ and $(\partial\mathscr{B})_{\mathrm{Right}}$. Finally, the boundary condition (71f) is introduced following Anand et al.[44].

To complete the mathematical formulation of the problem, we prescribe the initial conditions,

$$\chi^r(R, \Theta, Z, 0) = R, \tag{72a}$$

$$\chi^\vartheta(R, \Theta, Z, 0) = \Theta, \tag{72b}$$

$$\chi^z(R, \Theta, Z, 0) = Z, \tag{72c}$$

$$p(R, \Theta, Z, 0) = 0, \tag{72d}$$

$$\omega_{\mathrm{N}}(R, \Theta, Z, 0) = \omega_{\mathrm{Nenv}}, \tag{72e}$$

$$\gamma(R, \Theta, Z, 0) = 1, \tag{72f}$$

$$\omega_{\mathrm{p}}(R, \Theta, Z, 0) = 1, \tag{72g}$$

$$\varepsilon_{\mathrm{p}}(R, \Theta, Z, 0) = 0, \tag{72h}$$

$$\mathbf{e}_{\mathrm{p}}(R, \Theta, Z, 0) = 0, \tag{72i}$$

with $R \in [0, R_{\mathrm{b}}]$, $\Theta \in [0, 2\pi[$ and $Z \in [-L/2, L/2]$. The conditions (72a)–(72i) have to be valid in the whole domain $\mathscr{B}$.

The material parameters $k_{0\mathrm{R}}$, m_0, m_1, and $d_{0\mathrm{R}}$, the coefficients ζ_{pn}, ζ_{fp}, ζ_{nf}, and ζ_{Np} as well as the constants ω_{Nenv}, ω_{Ncr}, ω_{N0}, δ_1, δ_2, σ_{th}, and λ_{p} are given in Table 1 .

In Table 1 , the length of the cylindric specimen, L, and the radius of its cross section, R_{b}, are chosen within a plausible physical range. However, it is necessary to motivate the choice of the parameters ω_{Nenv}, ω_{Ncr}, and ω_{N0}, which are all taken from Di Stefano et al.[54]. These quantities are adapted from[24], where they were set equal to $\omega_{\mathrm{Nenv}} = 7.0 \cdot 10^{-6}$, $\omega_{\mathrm{Ncr}} = 2.0 \cdot 10^{-6}$, and $\omega_{\mathrm{N0}} = 4.2 \cdot 10^{-6}$, respectively. With the exception of ω_{Ncr}[4], in the work of Mascheroni et al.[24] these values come from experiments performed on tumour spheroids and associated with geometry, size, diffusion length scales and nutrients' characteristic mass fractions that are very different from those considered in our work. Indeed, an essential feature of the benchmark problem investigated by Mascheroni et al.[24] is that, because of the spherical geometry of the tumour, and because of the nutrients being distributed homogeneously on the tumour's surface, the diffusion of the nutrients occurs isotropically, from the boundary to the

[4]Note that the values attributed to ω_{Ncr} Mascheroni et al.[24] for all the considered studies are never referenced, the only exception being the growth of a tumour spheroid. In this case, however, the reference is a typographical error.

center of the spheroid, in radial direction. In our problem, instead, the nutrients can diffuse only along the axial direction of the tumour, and they have to travel the length L, which is much larger than the radius, of about 20 μm, of the spheroids considered Mascheroni et al.[24]. Due to these geometric and size aspects, if we used the values of ω_{Nenv}, ω_{Ncr} and ω_{N0} suggested Mascheroni et al., we would generate a situation in which the replenishment of the nutrients "eaten" by the cells would be too slow for the tumour to grow. Indeed, especially in the middle of the tumour, the nutrients' mass fraction would go below the threshold value, ω_{Ncr}, after few hours. Therefore, to avoid a fast inhibition of growth, we have increased the value of ω_{Nenv} of three orders of magnitude in our experiment *in silico*. Note that there is a certain freedom in the choice of ω_{Nenv}, since prescribing its value amounts to preparing the bath of nutrients in which the tumour is immersed. This freedom notwithstanding, the value assigned to ω_{Nenv} should take into account the characteristic length of the tumour —in our case, L— in order to ensure that the effects of growth remain active over a sufficiently long time scale. In principle, ω_{Ncr} and ω_{N0} should be determined experimentally. Still, since we are not aware of any experimental value of ω_{Ncr}, we have calibrated it so that ω_{Ncr} be smaller than ω_{Nenv}, but big enough to allow for a transition from the stage of tumour growth, for $\omega_{\mathrm{Ncr}} < \omega_{\mathrm{N}} \leq \omega_{\mathrm{Nenv}}$, to the stage of no growth, for $\omega_{\mathrm{N}} \leq \omega_{\mathrm{Ncr}} < \omega_{\mathrm{Nenv}}$. This reasoning has led us to choose ω_{Ncr} three orders of magnitude greater than the value assigned Mascheroni et al.[24]. Finally, the value given to ω_{N0} in our work (see Table 1) is two orders of magnitude greater than the one prescribed by Mascheroni et al.[24]. This choice allows us to be consistent with the scale of the nutrients' mass fraction imposed in our work.

6 | SOME COMPUTATIONAL ASPECTS

The system (65a)–(65h) features both ordinary differential equations (ODEs) in time, and partial differential equations (PDEs). All the ODEs of our model, including those obtained after that the finite element discretisation of the PDEs is performed, have been discretised adaptively in time, and have been solved by means of a four-step Backward Differentiation Formula (BDF4). This is an implicit linear multistep method, which generalises the implicit Euler method. Since the BDF4 is implicit, it requires in general the solution of nonlinear equations at each time integration step. The BDF4 is available in COMSOL Multiphysics®, which has been used to run our simulations.

The PDEs have been put in weak form and solved by means of Finite Element techniques. In particular, classical methods have been used for (65b), (65d), and (65h), while a "special treatment" has been reserved to the momentum balance law (65a), for which the Hu-Washizu method[76] has been employed.

Looking more closely at the PDEs (65b), (65d), and (65h), we notice that (65b) is a generalised Poisson equation in the pressure, p, with a time-dependent right-hand-side, $\dot{J}$, which represents the volume change of the solid phase due to the changes in porosity accompanying the flow of the fluid. Equation (65d), instead, is a nonlinear diffusion-advection-reaction equation in the mass fraction of the nutrients, ω_{N}, with the nonlinearity being nested in the reaction terms, R_{Np} and R_{s}. Both for (65b) and for (65d), the Finite Element Method leads to a set of ODEs in which the unknowns are the nodal pressures and the nodal mass fractions of the nutrients, respectively. Finally, Equation (65h) is an equation of Helmholtz type and, in this case, the Finite Element method yields a set of algebraic equations in the nodal values of $\mathbf{e}_{\mathrm{p}}$, which are anyway time-dependent. In the following, we do not fuss over the procedure for obtaining the set of nodal equations associated with (65b), (65d), and (65h), since such procedure is rather standard.

To sketch the formulation of the Hu-Washizu method, we add together the expressions of the stress tensors $\boldsymbol{P}_{\mathrm{f}}$ and $\boldsymbol{P}_{\mathrm{s}}$, and we notice that the weak form of the momentum balance law (65a) admits the compact form

$$\int_{\mathscr{B}} (\boldsymbol{P}_{\mathrm{f}} + \boldsymbol{P}_{\mathrm{s}}) : \boldsymbol{g}\,\mathrm{Grad}\,\boldsymbol{U}_{\mathrm{s}} = \int_{\mathscr{B}} \left(-J p\, \boldsymbol{g}^{-1} \boldsymbol{F}^{-\mathrm{T}} + \boldsymbol{P}_{\mathrm{sc}}\right) : \boldsymbol{g}\,\mathrm{Grad}\,\boldsymbol{U}_{\mathrm{s}} = 0, \tag{73}$$

where $\boldsymbol{U}_{\mathrm{s}}$ is the virtual velocity of the solid, expressed as a function of the points X of $\mathscr{B}$.

One of the main drawbacks of this formulation is that, once a Finite Element scheme is used for solving (73), the "limitations" of the interpolations adopted for χ[76], $\boldsymbol{F}$, and $\boldsymbol{F}_{\mathrm{p}}$ are transferred to $\boldsymbol{P}_{\mathrm{sc}}$ through its constitutive representation, $\hat{\boldsymbol{P}}_{\mathrm{sc}}(\boldsymbol{F}, \boldsymbol{F}_{\gamma}, \boldsymbol{F}_{\mathrm{p}})$. This ill behaviour persists even increasing the order of the basis functions used for the discretisation of χ, and may lead to a remarkable deterioration of the resolution of $\boldsymbol{P}_{\mathrm{sc}}$, with consequent loss of accuracy of the employed numerical method. A possible way to contain the occurrence of the just depicted numerical phenomenon is supplied by the Hu-Washizu method[76], which we implement for our purposes in its three-field-formulation. Although the Hu-Washizu method is well known in the computational community, we briefly explain here how we adapt it to the case under investigation in this work.

Together with the motion, χ, which is an unknown of the model, we introduce two tensor-valued auxiliary variables, which we regard as additional independent fields of our model: these are an auxiliary "deformation gradient tensor", $\boldsymbol{F}^{\mathrm{HW}}$, and an auxiliary first Piola-Kirchhoff stress tensor, $\boldsymbol{P}_{\mathrm{sc}}^{\mathrm{HW}}$ (note that the superscript "HW" stands for "Hu-Washizu"). Although being independent, $\boldsymbol{F}^{\mathrm{HW}}$ and $\boldsymbol{P}_{\mathrm{sc}}^{\mathrm{HW}}$ must be consistent with the *true* deformation gradient tensor and with the *true* first Piola-Kirchhoff stress tensor, respectively, and are thus bound to satisfy the constraints

$$\boldsymbol{F}^{\mathrm{HW}} = \boldsymbol{F}, \tag{74a}$$

$$\boldsymbol{P}_{\mathrm{sc}}^{\mathrm{HW}} = \boldsymbol{\mathcal{P}}_{\mathrm{sc}}(\boldsymbol{F}^{\mathrm{HW}}, \boldsymbol{F}_{\gamma}, \boldsymbol{F}_{\mathrm{p}}). \tag{74b}$$

To proceed with the Hu-Washizu method, we rephrase Equations (74a) and (74b) in weak form. Hence, we write

$$\int_{\mathscr{B}} \left\{ \left[\boldsymbol{F} - \boldsymbol{F}^{\mathrm{HW}} \right] : \boldsymbol{\Pi} + \left[\boldsymbol{\mathcal{P}}_{\mathrm{sc}}(\boldsymbol{F}^{\mathrm{HW}}, \boldsymbol{F}_{\gamma}, \boldsymbol{F}_{\mathrm{p}}) - \boldsymbol{P}_{\mathrm{sc}}^{\mathrm{HW}} \right] : \boldsymbol{\Lambda} \right\} = 0, \tag{75}$$

where $\boldsymbol{\Pi}$ and $\boldsymbol{\Lambda}$ denote the virtual variations of $\boldsymbol{P}_{\mathrm{sc}}^{\mathrm{HW}}$ and $\boldsymbol{F}^{\mathrm{HW}}$, respectively, and represent a virtual stress rate and a virtual velocity gradient. Equation (75) is now appended to (73), which has to be reformulated in terms of the Hu-Washizu auxiliary fields, thereby obtaining

$$\int_{\mathscr{B}} \left\{ \left[\boldsymbol{P}_{\mathrm{sc}}^{\mathrm{HW}} - (\det \boldsymbol{F}^{\mathrm{HW}}) p \boldsymbol{g}^{-1} (\boldsymbol{F}^{\mathrm{HW}})^{-\mathrm{T}} \right] : \boldsymbol{g} \operatorname{Grad} \boldsymbol{U}_{\mathrm{s}} + \left[\boldsymbol{F} - \boldsymbol{F}^{\mathrm{HW}} \right] : \boldsymbol{\Pi} + \left[\boldsymbol{\mathcal{P}}_{\mathrm{sc}}(\boldsymbol{F}^{\mathrm{HW}}, \boldsymbol{F}_{\gamma}, \boldsymbol{F}_{\mathrm{p}}) - \boldsymbol{P}_{\mathrm{sc}}^{\mathrm{HW}} \right] : \boldsymbol{\Lambda} \right\} = 0. \tag{76}$$

After performing the interpolation of all the fields introduced so far, the algebraic form of (76) consists of a block system, in which one block corresponds to the balance of momentum, one block is associated with (74a), and one with (74b).

7 | RESULTS

To weigh the effects of the non-local theory of remodelling on the benchmark problem presented in Section 5.2, we perform two different simulations: one is done by excluding micro-plasticity, and is thus said to be "standard"; the other one, instead, accounts for micro-plasticity, and refers to the "non-standard" model.

The standard model (ST) is obtained by setting A_{ν}, B_{ν}, and Z_{ν} equal to zero, so that Equation (65h) is always satisfied and the evolution law for ε_{p} only takes into account the first term of the right-hand-side of (65f), with $\boldsymbol{\Sigma}_{\nu} \equiv \boldsymbol{\Sigma}_{\nu}^{(\mathrm{st})}$. In the non-standard model (NST), the parameters A_{ν}, B_{ν}, and Z_{ν} are different from zero (see Table 2), and the full system of equations (65a)–(65h) has to be solved.

Since, to the best of our knowledge, no measurements for A_{ν}, B_{ν}, and Z_{ν} are available in the scientific literature on soft tissues, we have chosen such parameters after several trials. For this reason, the values used to obtain Figures 2 –5 may be unrealistic for describing a true biological situation. Moreover, we remark that the convergence of the system (65a)–(65h) was achieved only for $Z_{\nu} \leq 1$ and $A_{\nu} > B_{\nu}$, whereas our computations never converged for $Z_{\nu} > 1$, regardless of the tested values of A_{ν} and B_{ν}. We also emphasise that, for the cases in which the model converged, the results of the simulations featured no remarkable difference.

To report the results of our model, we display the numerical solutions of the displacement, the growth parameter, γ, the mass fraction of the proliferating cells, ω_{p}, the pressure, p, and the axial component of the effective Cauchy stress tensor, $\sigma_{\mathrm{eff}}^{zz}$. We plot all these quantities versus the axial coordinate of the specimen, and at the times $t = 10$ d and $t = 20$ d.

Figure 2 shows the displacement of the tumour (left panel) and the growth parameter, γ (right panel). Both quantities are computed only for the case of growth without "plasticity" (remodelling) (NP), i.e., for $\boldsymbol{F}_{\mathrm{p}} = \boldsymbol{I}$, $\varepsilon_{\mathrm{p}} = 0$, $\mathfrak{e}_{\mathrm{p}} = 0$, and for the case in which "plasticity" (remodelling) is active. Moreover, "plasticity" is accounted for as prescribed by the non-standard model (NST). In fact, we could have also used the standard one (ST), but it would have led to imperceptible differences with respect to the non-standard model. As expected, both the displacement and the growth parameter increase as time goes by, but we observe a drastic reduction of their spatiotemporal evolution when remodelling is active. The results presented in Figure 2 confirm the ones obtained by Mascheroni et al.[24] and Di Stefano et al.[54], and have been re-computed with the purpose of highlighting the important role that remodelling may play on growth.

To further investigate the possible role of remodelling on growth and, in particular, the switch from the standard to the non-standard approach, we study the evolution of ω_{p} (Figure 3), p (Figure 4), and $\sigma_{\mathrm{eff}}^{zz}$ (Figure 5).

TABLE 1 Numerical values of the parameters used both for the standard and for the non-standard model.

Parameter	Unit	Value	Equation	Reference
L	[cm]	1.000	—	[54]
R_b	[cm]	$1.000 \cdot 10^{-2}$	—	[54]
k_{0R}	[mm^4/(N s)]	0.4875	(67a)	[59]
m_0	[−]	0.0848	(67a)	[59]
m_1	[−]	4.6380	(67a)	[59]
d_{0R}	[m^2/s]	$3.200 \cdot 10^{-9}$	(67b)	[59]
σ_{th}	[Pa]	$1.000 \cdot 10^{-7}$	(58)	[32]
λ_p	[m s/kg]	$7.000 \cdot 10^{-7}$	(59)	[32]
λ	[Pa]	$1.333 \cdot 10^{4}$	(47)	[77]
μ	[Pa]	$1.999 \cdot 10^{4}$	(47)	[77]
ω_{Ncr}	[−]	$1.000 \cdot 10^{-3}$	(68a)	[54]
ω_{Nenv}	[−]	$7.000 \cdot 10^{-3}$	(68b)	[54]
ω_{N0}	[−]	$1.480 \cdot 10^{-4}$	(68e)	[54]
δ_1	[−]	$7.138 \cdot 10^{-1}$	(68b)	[78]
δ_2	[Pa]	$1.541 \cdot 10^{3}$	(68b)	[78]
ζ_{pn}	[kg/(m^3 s)]	$1.500 \cdot 10^{-3}$	(68a)	[79]
ζ_{fp}	[kg/(m^3 s)]	$1.343 \cdot 10^{-3}$	(68b)	[79]
ζ_{nf}	[kg/(m^3 s)]	$1.150 \cdot 10^{-5}$	(68d)	[79]
ζ_{Np}	[kg/(m^3 s)]	$3.000 \cdot 10^{-4}$	(68e)	[80]

Figure 3 displays, in the left panel, the progression of the mass fraction of the proliferating cells, ω_p, and, in the right panel, the absolute value of the difference between ω_p^{ST} and ω_p^{NST}, which denote the mass fractions of the proliferating cells computed with the standard model (ST) and the non-standard model (NST), respectively. In the left panel, we notice that, at time $t = 10$ d, the differences between ω_p^{ST} and ω_p^{NST} are irrelevant. However, at $t = 20$ d, a slight, yet appreciable, difference starts to appear. We visualise this difference in the right panel of Figure 3 . Here, we notice that, due to the Dirichlet boundary condition imposed on ω_p at $Z = L/2$, such difference cannot be pronounced for values of the axial coordinate tending to $L/2$. On the other hand, $|\omega_p^{ST} - \omega_p^{NST}|$ becomes relatively more visible in the portion of the specimen in which growth is inhibited (see Figure 2 (right)). This is due to a limited availability of nutrients (data not shown).

In the left panel of Figure 4 , we show the pressure, p, both for the ST model and for the NST one. For both models, the same behaviour is attained, i.e., the pressure drops from the tumour boundary towards its centre, where it takes negative values. In the right panel of Figure 4 , we report the absolute value of the difference, at time $t = 20$ d, between p^{ST} and p^{NST}, i.e., the pressures computed with the ST model and the NST model, respectively. The differences between p^{ST} and p^{NST} are relatively small, but visible, in almost all of the half domain and at both times. They are clearly zero at the Dirichlet boundary $Z = L/2$ and, at $t = 20$ d, the maximum of $|p^{ST} - p^{NST}|$ is reached at a point between 0.4 cm and 0.5 cm.

Moreover, in Figure 5 , the axial component of the constitutive part of the Cauchy stress tensor, σ_{sc}^{zz}, is shown. Indeed, due to the imposed boundary conditions and the symmetry restrictions of the considered problem, the balance of momentum (65a) amounts to requiring $-p + \sigma_{sc}^{zz} = 0$ everywhere in the specimen. Hence, it holds that $\sigma_{sc}^{zz} = p$. In addition, the axial component of the stress used to model the mechanotransduction, σ_{eff}^{zz}, is different from σ_{sc}^{zz}, as it features $\partial \mathrm{e}_p / \partial Z$ (see Equation (70)). However, since this derivative is very small, it occurs that σ_{eff}^{zz} can be safely approximated with σ_{sc}^{zz} and, thus, with p.

A last comment concerns the evolution of e_p and ε_p. As reported in Figure 6 , both ε_p and e_p are increasing functions of time and space. If we focus on ε_p, we note that, as time goes by, the remodelling strains augment and accumulate in a neighbourhood of the boundaries of the specimen. This is highlighted by the fact that the slope of the curves corresponding to ε_p tends to raise when it approaches the edge. However, as predicted by the theory, e_p plays a smoothing role on the remodelling distortions and, in fact, it distributes itself more uniformly along the specimen. A relevant aspect of this result is that, while the curves corresponding to ε_p at $t = 10$ d and $t = 20$ d are almost coincident at the centre of the specimen, the curves determining e_p are distinguishable from one another.

TABLE 2 Numerical values of the parameters A_ν, B_ν and Z_ν for the non-standard model.

Parameter	Unit	Value	Equation
A_ν	[Pa]	$1.0 \cdot 10^{-9}$	(38c)
B_ν	[Pa m^2]	$1.0 \cdot 10^{-14}$	(38d)
Z_ν	[Pa]	$1.0 \cdot 10^{-2}$	(65f)

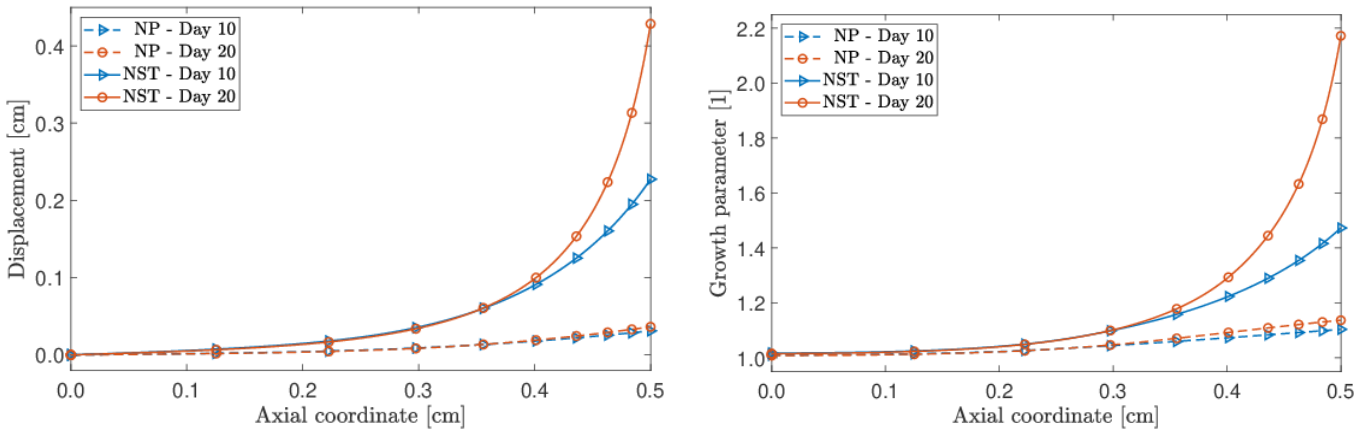

FIGURE 2 *Left panel*: spatial profile of the displacement. *Right panel*: spatial profile of the growth parameter, γ. Since the problem is symmetric, in both panels only the half $[0, L/2]$ of the domain is shown.

8 | CONCLUSIONS

In this work, we study an idealised biological tissue that grows and remodels. As tissue we consider a tumour in avascular stage, and we assume that its remodelling —or structural reorganisation— occurs through a two-scale plasticity-like phenomenon. Following [44], we distinguish a coarse and a fine scale, and we resolve this phenomenon, at the coarse scale, by means of the accumulated remodelling strain, ε_p, and, at the fine scale, by means of $\mathfrak{e}_p$. The latter is the representative of the so-called *micro-"plasticity"* and, being related to ε_p through a Helmholtz-like equation, it makes ε_p non-local [44]. Within this framework, we have set ourselves the scope of evaluating if, how, and to what extent the micro-"plasticity" influences the growth of the tumour. In our approach, such influence can occur both directly and indirectly. The direct way is due to the fact that the *effective* Cauchy stress, $\boldsymbol{\sigma}_{\text{eff}}$, modulates the source of mass R_{fp}, and thus also R_s, by giving rise to mechanotransduction. The indirect way, instead, manifests itself through the slight, and to a certain extent visible, changes that the non-local plastic-like distortions induce in some of the physical quantities that characterise the growth of the tumour, as reported in Section 7.

It is important to emphasise that the results shown in this work (see Figures 2 –5) are obtained for numerical values of the "non-standard" parameters A_ν, B_ν, and Z_ν (see Table 2), which could be far beyond the physical range. Therefore, for the time being, our results aim at being a qualitative contribution to a unified strain-gradient theory of growth and remodelling. However, they are quantitative in evaluating the impact of the considered theory on growth.

We remark that, following an idea put forward by Epstein [81], Di Stefano et al. [54] proposed a model of strain-gradient growth, in which the evolution of γ is governed by a generalised diffusion-reaction equation. Such equation was obtained by accounting

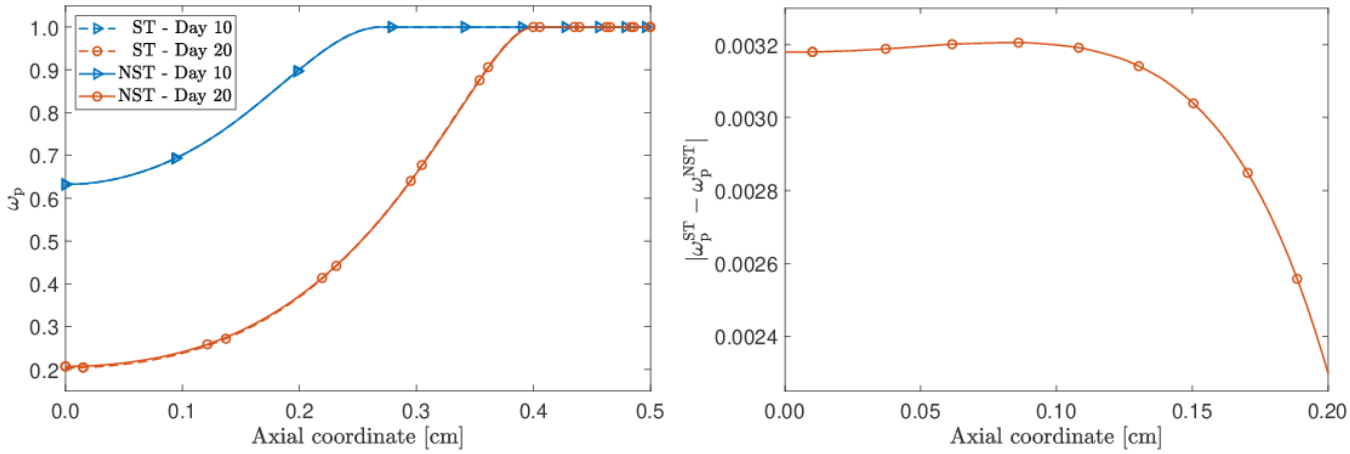

FIGURE 3 *Left panel*: spatial profile of the mass fraction of the proliferating cells, ω_p. Since the problem is symmetric, only the half $[0, L/2]$ of the domain is shown. *Right panel*: spatial profile of the absolute value of the difference between ω_p^{ST} and ω_p^{NST}, i.e., the mass fractions of the proliferating cells computed with the standard model (ST) and the non-standard model (NST), respectively. The picture refers to the portion of the half domain in which $|\omega_p^{ST} - \omega_p^{NST}|$ is greater than, approximatively, $2.25 \cdot 10^{-3}$, and is computed at time $t = 20$ day.

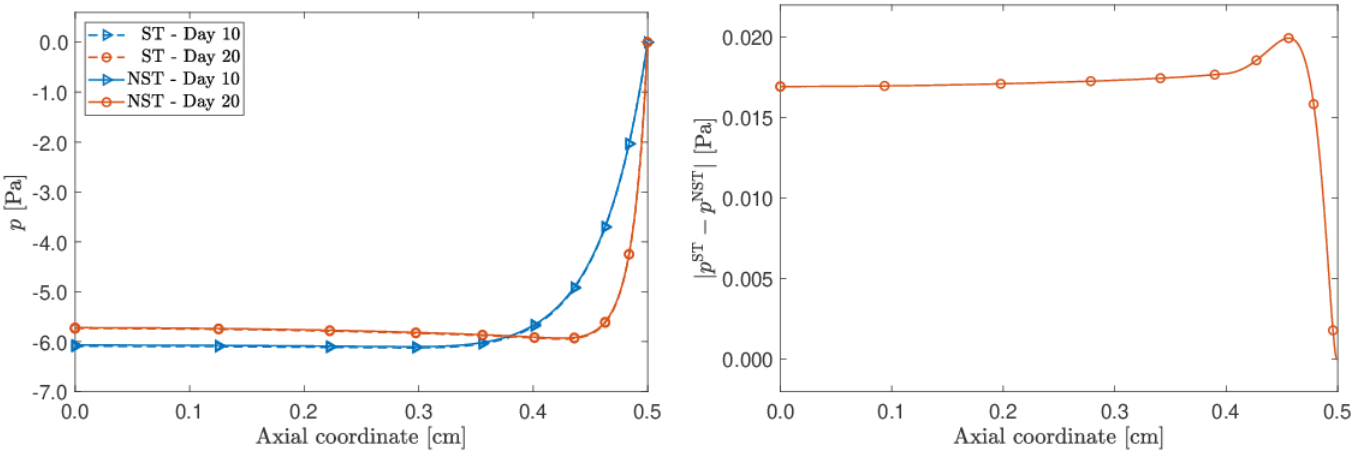

FIGURE 4 *Left panel*: spatial profile of the pressure, p. *Right panel*: spatial profile of the absolute value of the difference between p^{ST} and p^{NST}, which denote the pressure computed with the standard model (ST) and the pressure computed with the non-standard model (NST). The picture is computed at time $t = 20$ day. Since the problem is symmetric, in both panels only the half $[0, L/2]$ of the domain is shown.

for the growth-induced scalar curvature, κ_γ[5], which features the spatial derivatives of γ up to the second order. However, in that model we considered no remodelling. In the present work, instead, we have neglected the role of κ_γ, but we have focussed our attention on strain-gradient remodelling in order to quantify its effect on growth. The role of κ_γ in the current framework can be recovered by simply re-activating $r_{p\gamma}$ and $r_{n\gamma}$ in (2a) and (2b) (see Di Stefano et al.[54] for the definition of these terms as functions of κ_γ).

Apart from the obvious fact that the topics under study necessitate further investigations from our side, two comments are in order: firstly, we have not hypothesised a strain-softening behaviour of the considered material, and no formation of shear

[5]The growth distortions, $\boldsymbol{F}_\gamma = \gamma \boldsymbol{I}$, induce the Riemannian metric tensor $\boldsymbol{C}_\gamma = \gamma^2 \boldsymbol{G}$, which yields Christoffel symbols that allow to determine a Levi-Civita connection with nontrivial fourth-order curvature tensor[61,66] and, thus, with nontrivial associated Ricci curvature tensor, $\mathfrak{R}_\gamma$. Hence, it is possible to define the scalar curvature as $\kappa_\gamma := \mathfrak{R}_\gamma : \boldsymbol{C}_\gamma^{-1}$ (see[54] for details).

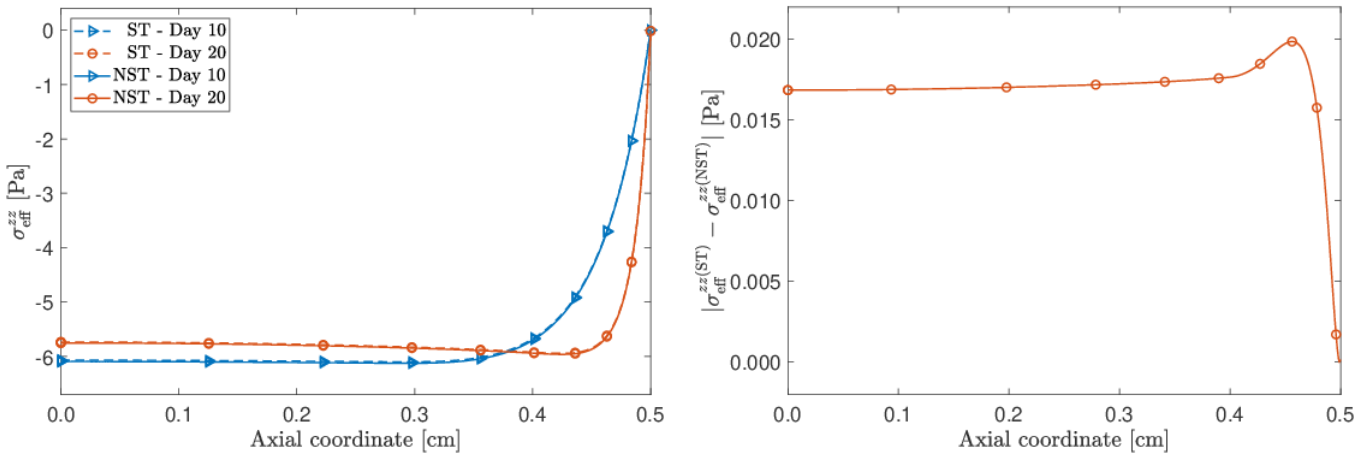

FIGURE 5 *Left panel*: spatial profile of the axial component of the effective Cauchy stress tensor, $\sigma^{zz}_{\rm eff}$. *Right panel*: spatial profile of the absolute value of the difference between $\sigma^{zz(\rm ST)}_{\rm eff}$ and $\sigma^{zz(\rm NST)}_{\rm eff}$, which denote the stress computed with the standard model (ST) and the non-standard model (NST), respectively. The picture is computed at time $t = 20$ day. Since the problem is symmetric, in both panels only the half $[0, L/2]$ of the domain is shown.

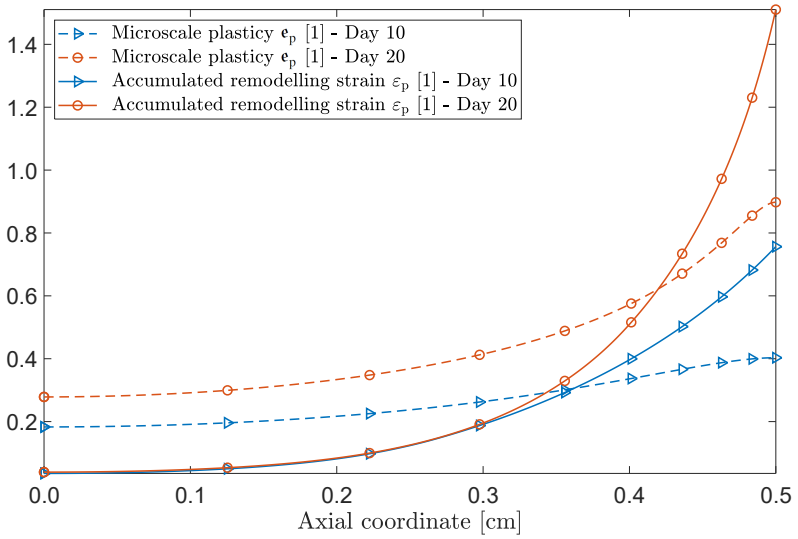

FIGURE 6 Spatial profiles of the accumulated remodelling strain $\varepsilon_{\rm p}$ and of the microscale plasticity $\mathbf{e}_{\rm p}$. Since the problem is symmetric, only the half $[0, L/2]$ of the domain is shown.

bands can be observed that justifies from the outset the use of a strain-gradient regularisation; secondly, the benchmark problem adopted in this work might be inappropriate, since it does not produce the desired/expected localisation of the accumulated plastic strain, $\varepsilon_{\rm p}$, which calls for the employment of a strain-gradient theory. Nevertheless, our model is able to capture the regularising effect that the microscale descriptor $\mathbf{e}_{\rm p}$ has on the accumulated remodelling distortions (cf. Figure 6).

It is known that the internal structural changes occurring in heterogeneous materials influence their overall macroscopic behaviour. For example, in bones, the change of orientation of the lamellae's collagen fibres modifies the bone's longitudinal effective Young's modulus[82,83]. In the present work, we attempt to know how, and to what extent, the microscopic plastic-like (remodelling) effects are significant for the macroscopic evolution of the tissue. To the best of our knowledge, there are no experimental studies showing the influence of the microscopic plastic effects on the tissue behaviour. However, one can think of an experiment where, at some level, there can be a relatively strong localisation of the accumulated "plastic" strain, $\mathbf{e}_{\rm p}$, because of the presence of constraints (e.g. contact of the tissue with much stiffer materials). In this respect, we hope that our work

contributes to understand the interactions between growth and remodelling by merging the theories of multiphasic materials and of strain-gradient plasticity.

To the best of our understanding, another important difference between our work and previous publications (see e.g. [39–41]) resides in the definition of the internal and external mechanical powers. Indeed, looking for instance at [40], these powers feature only the generalised velocities associated with the "classical" degrees of freedom of a body[6], while the time derivatives of the tensors associated with the body's structural changes appear in the study of the dissipation inequality through the derivative of the body's Helmholtz free energy density. In our case, instead, following a philosophy outlined in other papers [29,44,45,52,64], we introduce the structural kinematic descriptors both constitutively, i.e., as arguments of the solid phase Helmholtz free energy density, and in the formulation of the overall virtual powers of the problem, that is, jointly with the "classical" ones.

In our work, the tensor $\tilde{\boldsymbol{\Sigma}}_\nu$ is entirely determined by mechanical quantities (cf. Equation (38a)) and this property is inherited by its associated direction tensor, $\boldsymbol{N}_\nu = \tilde{\boldsymbol{\Sigma}}_\nu / \|\tilde{\boldsymbol{\Sigma}}_\nu\|_{\boldsymbol{\eta}}$. Consequently, the hypothesis of co-directionality of $\tilde{\boldsymbol{D}}_\mathrm{p}$ and $\tilde{\boldsymbol{\Sigma}}_\nu$ implies that the direction of the plastic flow is exclusively dictated by mechanical stress, the latter being augmented by the non-standard contribution $\tilde{\boldsymbol{\Sigma}}_\nu^{(\text{n-st})}$. However, in more general situations, it is possible to define generalised Mandel stress tensors featuring bio-chemical contributions, i.e., depending explicitly on the mass fraction of the nutrients (and on its gradient). In such cases, tensor $\boldsymbol{N}_\nu$ defines the direction of the plastic flow on the basis of chemo-mechanical guidance.

A last comment is on the design of an adequate benchmark problem. Indeed, when Anand et al. [44] developed their theory, they wrote that $\mathbf{e}_\mathrm{p}$ *"is introduced for the purpose of regularisation of numerical simulations of shear band formation under strain softening conditions"*. To achieve this objective, they called for the concept of micro-scale plasticity, and admitted a physics described by ε_p, $\mathbf{e}_\mathrm{p}$, and $\mathrm{Grad}\mathbf{e}_\mathrm{p}$. Then, in order to determine these quantities, they established a thermodynamically consistent framework, rather than simply improving the equations that were problematic from the numerical point of view. In our work, we have extended such thermodynamic set-up to a growth problem, by admitting that its physical meaning goes beyond the necessity of solving numerical issues. Nevertheless, we have seen only a very marginal impact of this modelling choice on our results and we argue that it is of fundamental importance to design benchmark problems capable of capturing the physics behind it. This is part of our ongoing research.

ACKNOWLEDGMENTS

We kindly acknowledge the *Dipartimento di Scienze Matematiche* (DISMA) "G.L. Lagrange" of the *Politecnico di Torino*, *"Dipartimento di Eccellenza 2018–2022"* ('Department of Excellence 2018–2022'), Project code: E11G18000350001. Our warmest thanks go to Luigi Preziosi and Chiara Giverso (DISMA, *Politecnico di Torino*) for precious discussions on the mass sources and for providing crucial references. AG thanks Salvatore Federico, the person with whom he moved his first steps in Continuum Mechanics.

Author contributions

All Authors have equally contributed to this work.

Financial disclosure

ART's post-doctoral scholarship is financed, in part, by the Doctoral School of the *Politecnico di Torino* and, in part, by the *Dipartimento di Scienze Matematiche "Dipartimento di Eccellenza 2018–2022"* of the *Politecnico di Torino*, Project code: E11G18000350001.

Conflict of interest

The authors declare no potential conflict of interests.

[6] These are the body velocity, $\boldsymbol{V}$, the time derivative of the deformation gradient tensor, $\dot{\boldsymbol{F}}$, and the time derivative of the second gradient of the deformation, i.e., $\dot{\overline{\mathrm{Grad}\boldsymbol{F}}}$ [40].

SUPPORTING INFORMATION

None.

References

[1] L.A. Taber, *Applied Mechanics Reviews* **1995**, *48* (8), 487.

[2] Y.C. Fung, *Biomechanics. Motion, flow, stress, and growth*, Springer, New York, **1990**.

[3] S.C. Cowin, *J Biomech Eng* **2000**, *122*, 553–569.

[4] D. Ambrosi, L. Preziosi, *Biomechanics and Modeling in Mechanobiology* **2009**, *8*, 397–413.

[5] L. Preziosi, D. Ambrosi, C. Verdier, *J. Theor. Biol.* **2010**, *262(1)*, 35–47.

[6] C. Giverso, L. Preziosi, *Math. Med. Biol.* **2012**, *29(2)*, 181–204.

[7] R.A. Foty, C.M. Pfleger, G. Forgacs, M.S. Steinberg, *Development* **1996**, *122*, 1611–1620.

[8] G. Forgacs, R.A. Foty, Y. Shafrir, M.S. Steinberg, *Biophysical Journal* **1998**, *74*, 2227–2234.

[9] L. Preziosi, G. Vitale, *Math. Models Methods Appl. Sci.* **2011**, *21* (09), 1901–1932.

[10] N.J.B. Driessen, W. Wilson, C.V.C. Bouten, F.P.T. Baaijens, *J. Theor. Biol.* **2004**, *226*, 53–64.

[11] I. Hariton, G. de Botton, T.C. Gasser, G.A. Holzapfel, *Biomech. Model. Mechanobiol.* **2007**, *6(3)*, 163–175.

[12] A. Menzel, *Biomechan. Model. Mechanobiol.* **2007**, *6(5)*, 303–320.

[13] T. Olsson, A. Klarbring, *Eur. J. Mech. A* **2008**, *27(6)*, 959–974.

[14] W. Wilson, N.J.B. Driessen, C.C. van Donkelaar, K. Ito, *Osteoarthr. Cartil.* **2006**, *14*, 1196–1202.

[15] T.M. Quinn, V. Morel, *Biomech. Model. Mechanobiol.* **2007**, *6*, 73–82.

[16] F. Baaijens, C. Bouten, N. Driessen, *J. Biomech.* **2010**, *43*, 166–175.

[17] A. Grillo, G. Wittum, A. Tomic, S. Federico, *Math. Mech. Solids* **2015**, *20(9)*, 1107–1129.

[18] A. Grillo, M. Carfagna, S. Federico, *J. Eng. Math.* **2018**, *109(1)*, 139–172.

[19] E. Crevacore, S. Di Stefano, A. Grillo, *International Journal of Nonlinear Mechanics* **2018**, *In press*.

[20] D. Garcia, P.K. Zysset, M. Charlebois, A. Curnier, *Biomech. Model. Mechanobiol.* **2009**, *8(2)*, 149–165.

[21] J. Lubliner, *Plasticity Theory*, Dover Publications, Inc., Mineola, New York, **2008**.

[22] M.V. Mićunović, *Thermomechanics of Viscoplasticity*, Springer New York, **2009**.

[23] P. Ciarletta, D. Ambrosi, G.A. Maugin, L. Preziosi, *Eur. Phys. J. E* **2013**, *36*, 23.

[24] P. Mascheroni, M. Carfagna, A. Grillo, D.P. Boso, B.A. Schrefler, *Mathematics and Mechanics of Solids* **2018**, *23* (4), 686–712.

[25] W. Ehlers, K. Bircher, A. Stracuzzi, V. Marina, M. Zündel, E. Mazza, *Nat. Commun.* **2017**, *1002(8)*, 1–10.

[26] A. Menzel, E. Kuhl, *Mechanics Research Communications* **2012**, *42*, 1–14.

[27] M. Epstein, G.A. Maugin, *International Journal of Plasticity* **2000**, *16* (7-8), 951–978.

[28] V.A. Lubarda, A. Hoger, *International Journal of the Mechanics and Physics of Solids* **2002**, *39*, 4627–4664.

[29] A. Di Carlo, S. Quiligotti, *Mechanics Research Communications* **2002**, *29* (6), 449–456.

[30] M. Epstein, *The geometric language of continuum mechanics*, Cambridge University Press, **2010**.

[31] M. Epstein, M. Elżanowski, *Material Inhomogeneities and their Evolution — A Geometric Approach 1st ed.*, Springer-Verlag Berlin Heidelberg, **2007**.

[32] A. Grillo, R. Prohl, G. Wittum, *Continuum Mech. Therm.* **2016**, *28*, 579–601.

[33] H. Byrne, L. Preziosi, *Mathematical Medicine and Biology* **2003**, *20* (4), 341–366.

[34] G.A. Ateshian, *Biomechanics and Modeling in Mechanobiology* **2007**, *6* (6), 423–445.

[35] D. Ambrosi, L. Preziosi, G. Vitale, *Z. Angew. Math. Phys.* **2010**, *61*, 177–191.

[36] A. Grillo, S. Federico, G. Wittum, *Int. J. Nonlinear Mech.* **2012**, *47*, 388–401.

[37] C. Giverso, M. Scianna, A. Grillo, *Mech. Res. Commun.* **2015**, *68*, 31–39.

[38] T. Stylianopoulos, J.D. Martin, V.P. Chauhan, S.R. Jain, et al., *PNAS* **2012**, *109(38)*, 15101–15108.

[39] P. Ciarletta, G.A. Maugin, *Int. J. Non-Lin. Mech.* **2011**, *46*, 1341–1346.

[40] P. Ciarletta, D. Ambrosi, G.A. Maugin, *J. Mech. Phys. Solids* **2012**, *60*, 432–450.

[41] P. Ciarletta, D. Ambrosi, G.A. Maugin, *Bulletin of the Polish Academy of Sciences –Technical Sciences* **2012**, *60(2)*, 253–257.

[42] D. Ambrosi, L. Preziosi, G. Vitale, *Mech. Res. Commun.* **2012**, *42*, 87–91.

[43] M.E. Gurtin, E. Fried, L. Anand, *The Mechanics and Thermodynamics of Continua*, Cambridge University Press, **2010**.

[44] L. Anand, O. Aslan, A. Chester, *International Journal of Plasticity* **2012**, *30–31*, 116–143.

[45] M.E. Gurtin, L. Anand, *International Journal of Plasticity* **2005**, *21*, 2297–2318.

[46] L. Anand, M.E. Gurtin, S.P. Lele, C. Gething, *Journal of the Mechanics and Physics of Solids* **2005**, *53*, 1789–1826.

[47] E.C. Aifantis, *Transactions on ASME Journal of Engineering Materials and Technology* **1984**, *106*, 326–330.

[48] E.C. Aifantis, *International Journal of Plasticity* **1987**, *3*, 211–247.

[49] A. Madeo, F. dell'Isola, F. Darve, *Journal of the Mechanics and Physics of Solids* **2013**, *61(11)*, 2196–2211.

[50] I. Giorgio, U. Andreaus, F. dell'Isola, T. Lekszycki, *Extreme Mechanics Letters* **2017**, *13*, 141–147.

[51] F. dell'Isola, A. Della Corte, I. Giorgio, *Mathematics and Mechanics of Solids* **2017**, *22(4)*, 852–872.

[52] M.E. Gurtin, *Physica D* **1994**, *92*, 178–192.

[53] D. Ambrosi, L. Preziosi, *Mathematical Models and Methods in Applied Sciences* **2002**, *12* (05), 737–754.

[54] S. Di Stefano, A. Ramírez-Torres, R. Penta, A. Grillo, *International Journal of Non-Linear Mechanics* **2018**, *106*, 174–187.

[55] C.J. Cyron, J.D. Humphrey, *Meccanica* **2017**, *52(3)*, 645–664.

[56] A. Tomic, A. Grillo, S. Federico, *IMA J. Appl. Math.* **2014**, *79*, 1027–1059.

[57] S. Quiligotti, *Theoret. Appl. Mech.* **2002**, *28-29*, 277–288.

[58] S. Quiligotti, G.A. Maugin, F. dell'Isola, *Acta Mech.* **2003**, *160*, 45–60.

[59] M.H. Holmes, V.C. Mow, *Journal of biomechanics* **1990**, *23*, 1145–1156.

[60] J. Bear, Y. Bachmat, *Introduction to Modeling of Transport Phenomena in Porous Media*, Kluwer, Dordrecht, **1990**.

[61] J.E. Marsden, T.J.R. Hughes, *Mathematical Foundations of Elasticity*, Dover Publications, Inc., Mineola, New York, **1983**.

[62] R.K. Jain, J.D. Martin, T. Stylianopoulos, *Annual Review of Biomedical Engineering* **2014**, *16*, 321–346.

[63] V. Ciancio, M. Dolfin, M. Francaviglia, S. Preston, *J. Non-Equilib. Thermodyn.* **2008**, *33(3)*, 199–234.

[64] P. Cermelli, E. Fried, S. Sellers, *Proc. R. Soc. Lond. A* **2001**, *457*, 1447–1467.

[65] S. Sadik, A. Yavari, *Mathematics and Mechanics of Solids* **2017**, *22* (4), 771–772.

[66] A. Goriely, *The Mathematics and Mechanics of Biological Growth*, Springer New York, **2016**.

[67] P. Haupt, *Continuum Mechanics and Theory of Materials*, Springer, **2000**.

[68] S. Pezzuto, D. Ambrosi, *International Journal for Numerical Methods in Biomedical Engineering* **2014**, *30(12)*, 1578–1596.

[69] B. Loret, F.M.F. Simões, *Eur. J. Mech. A* **2005**, *24*, 757–781.

[70] G. Sciarra, G.A. Maugin, K. Hutter, *Archive of Applied Mechanics* **2003**, *73*, 194–224.

[71] S.M. Hassanizadeh, *Adv. Water Resour.* **1986**, *9*, 207–222.

[72] L.S. Bennethum, M.A. Murad, J.H. Cushman, *Transport in Porous Media* **2000**, *39* (2), 187–225.

[73] I.S. Liu, *Archive Rational Mech. Anal.* **1972**, *46*, 131–148.

[74] G.A. Ateshian, J.A. Weiss, *J. Biomech. Engng.* **2010**, *132*, 111004–1–111004–7.

[75] S. Federico, A. Grillo, *Mech. Mater.* **2012**, *44*, 58–71.

[76] J. Bonet, R.D. Wood, *Nonlinear Continuum Mechanics for Finite Element Analysis*, Cambridge University Press, New York, **2008**.

[77] T. Stylianopoulos, J.D. Martin, M. Snuderl, F. Mpekris, S.R. Jain, R.K. Jain, *Cancer Research* **2013**, *73* (13), 3833–3841.

[78] P. Mascheroni, C. Stigliano, M. Carfagna, D.P. Boso, L. Preziosi, P. Decuzzi, B.A. Schrefler, *Biomech. Model. Mechanobiol.* **2016**, *15* (5), 1215–1228.

[79] M.A.J. Chaplain, L. Graziano, L. Preziosi, *Mathematical Medicine and Biology: A Journal of the IMA* **2006**, *23* (3), 197–229.

[80] J.J. Casciari, S.V. Sotirchos, R.M. Sutherland, *Cell Proliferation* **1992**, *25* (1), 1–22.

[81] M. Epstein in *Mechanics of Material Forces. Advances in Mechanics and Mathematics*, *Vol. 11*, Maugin G.A. Steinmann P. (Ed.), Springer, Boston, MA, **2005**, pp. 129–139.

[82] T.J. Vaughan, C.T. McCarthy, L.M. McNamara, *Journal of the Mechanical Behavior of Biomedical Materials* **2012**, *12*, 50–62.

[83] A. Ramírez-Torres, R. Penta, R. Rodríguez-Ramos, et al., *International Journal of Solids and Structures* **2018**, *130-131*, 190–198.

AUTHOR BIOGRAPHY

Alfio Grillo. AG is currently Associate Professor of Mathematical Physics at the *Politecnico di Torino*; his main scientific interests are Continuum and Theoretical Mechanics. **Salvatore Di Stefano.** SDiS is currently PhD student at the *Politecnico di Torino*; his main scientific interests are Continuum Mechanics and Differential Geometry. **Ariel Ramírez Torres.** ART is currently a post-doctoral fellow at the *Politecnico di Torino*; his main scientific interests are Continuum Mechanics and Asymptotic Homogenisation. **Michele Loverre.** ML is a former graduate student of the *Politecnico di Torino*; his main scientific interests are Continuum and Computational Mechanics. Part of the material presented in this work has been used in his MSc Thesis.

How to cite this article: A. Grillo, S. Di Stefano, A. Ramírez-Torres, and M. Loverre (2018), A study of growth and remodelling in isotropic tissues, based on the Anand-Aslan-Chester theory of strain-gradient Plasticity, *GAMM*, *Submitted*.